

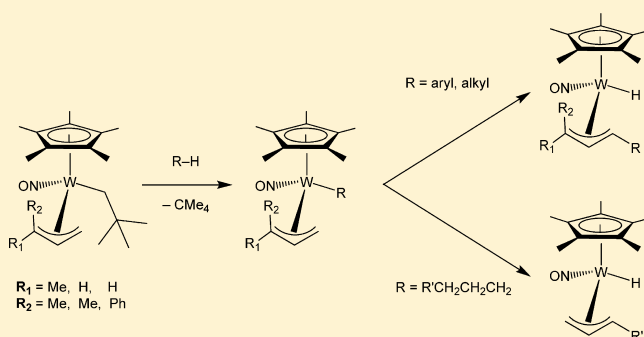
Factors Influencing the Outcomes of Intermolecular C–H Activations of Hydrocarbons Initiated by CpW(NO)(CH₂CMe₃)(η^3 -allyl) Complexes (Cp = η^5 -C₅Me₅ (Cp*), η^5 -C₅Me₄H (Cp'))

Rhett A. Baillie, Tommy Tran, Kathryn M. Lalonde, Jenkins Y. K. Tsang, Michelle E. Thibault, Brian O. Patrick, and Peter Legzdins*

Department of Chemistry, The University of British Columbia, Vancouver, British Columbia, Canada V6T 1Z1

Supporting Information

ABSTRACT: Gentle thermolyses of CpW(NO)(CH₂CMe₃)-(η^3 -allyl) complexes (Cp = η^5 -C₅Me₅ (Cp*), η^5 -C₅Me₄H (Cp')) in neat hydrocarbon solutions result in the loss of neopentane from the metal's coordination spheres and the transient formation of the 16-electron (16e) intermediate species CpW(NO)(η^2 -allene) and/or CpW(NO)(η^2 -diene). These transient intermediates can react with hydrocarbon substrates, RH (R = alkyl, aryl), to form three different types of organometallic products. The first products are the desired CpW(NO)(η^3 -allyl)(η^1 -R) complexes that result from the selective single activation of a C–H bond of RH. The second class of products involves CpW(NO)(H)(η^3 -(R)-allyl) complexes that are isomers of the CpW(NO)(η^3 -allyl)(η^1 -R) compounds resulting from an intramolecular R/allyl H exchange. Finally, the third type of products contains CpW(NO)(H)(η^3 -hydrocarbyl) species that result from three successive C–H activations of hydrocarbon substrates such as R'CH₂CH₂CH₃ and loss of the original allyl ligand. Just which organometallic products ultimately result from the reactions of the CpW(NO)(CH₂CMe₃)(η^3 -allyl) complexes with hydrocarbons depends on several factors, including the natures of the cyclopentadienyl and allyl ligands, the hydrocarbon substrates themselves, the electron density at the metal centers, and the experimental conditions employed. This article documents these dependences and identifies the optimum CpW(NO)(CH₂CMe₃)(η^3 -allyl) compounds and experimental conditions for effecting the selective single C–H bond activations of hydrocarbon substrates such as benzene as a representative arene and methylcyclohexane as a representative alkane. During the course of these investigations all new organometallic complexes have been characterized by conventional spectroscopic methods, and the solid-state molecular structures of several of them have been established by single-crystal X-ray crystallographic analyses.



INTRODUCTION

Current interest in effecting the activation and functionalization of hydrocarbon C–H bonds continues to be motivated by the long-term goal to develop new synthetic pathways to a broad range of industrially important products beginning with unfunctionalized starting materials.¹ Our recent contributions to this area of chemistry have involved the family of Cp*W(NO)(alkyl)(η^3 -allyl) (Cp* = η^5 -C₅Me₅) complexes,² which initiate various types of C–H activations. However, a more complete understanding of the mechanisms of these activations is required before these organometallic nitrosyl complexes can be utilized productively by synthetic chemists for the selective functionalization of C–H bonds.³ Specifically, explanations must first be found for the strikingly differing reactivities exhibited by various members of this family of compounds even though similar C–H-activating intermediate complexes are involved. For instance, as summarized in Scheme 1, the dimethylallyl complex Cp*W(NO)(CH₂CMe₃)(η^3 -CH₂CHCMe₂) effects the clean activation of a benzene C–H

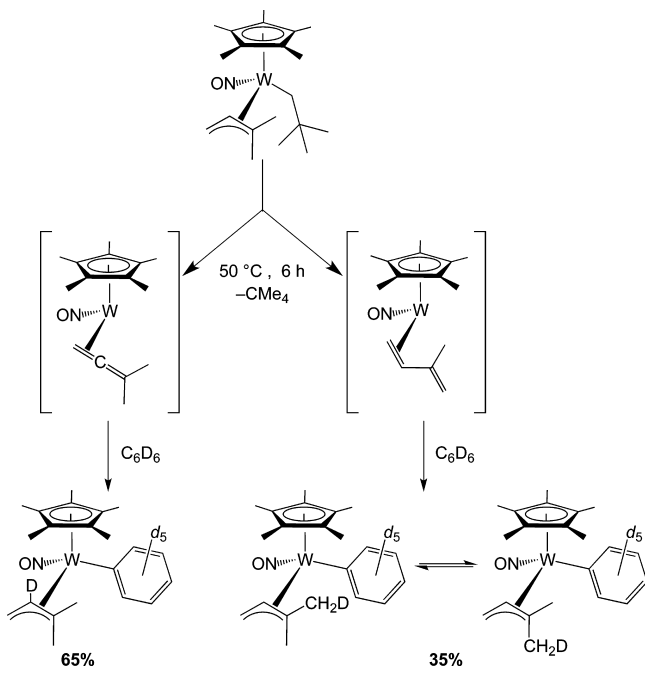
bond at 50 °C via η^2 -allene and η^2 -diene intermediate complexes and forms the expected phenyl complex Cp*W(NO)(Ph)(η^3 -CH₂CHCMe₂) in good yields.⁴ In contrast, thermolyses of the dimethylallyl compound in alkane solvents appear to afford mixtures of allyl hydride complexes resulting from three successive C–H bond activations at different places on the alkanes following loss of the original 1,1-dimethylallyl ligand.⁴

The situation is reversed for the monomethylallyl compound Cp*W(NO)(CH₂CMe₃)(η^3 -CH₂CHCHMe) and the phenylallyl complex Cp*W(NO)(CH₂CMe₃)(η^3 -CH₂CHCHPh) (Scheme 2). In the presence of linear alkanes, both compounds initiate sp³ C–H activations of the hydrocarbons exclusively at their terminal carbon atoms and cleanly form Cp*W(NO)(η -alkyl)(η^3 -CH₂CHCHR) (R = Me, Ph) complexes via either an η^2 -diene or an η^2 -allene intermediate complex.^{5,6} In contrast,

Received: November 15, 2011

Published: January 20, 2012

Scheme 1



the monomethylallyl compound loses neopentane at ambient temperatures in benzene solutions and forms a brown solution that contains a “complex mixture of organometallic compounds”.⁵

These observations clearly indicate that it is not the nature of the 16e intermediate formed by thermolysis of the $\text{Cp}^*\text{W}(\text{NO})(\text{alkyl})(\eta^3\text{-allyl})$ precursor complex that determines the eventual outcomes of the C–H activations initiated by that complex. Consequently, we decided to investigate these $\text{Cp}^*\text{W}(\text{NO})(\text{CH}_2\text{CMe}_3)(\eta^3\text{-allyl})$ systems more fully with a view to finding the explanations for their differing chemical behaviors, particularly why some C–H activations produce just a single organometallic product whereas others afford a plethora of products. In this article we present the results of our investigations, which in some cases have been extended to encompass the Cp' analogues ($\text{Cp}' = \eta^5\text{-C}_5\text{Me}_4\text{H}$) of these

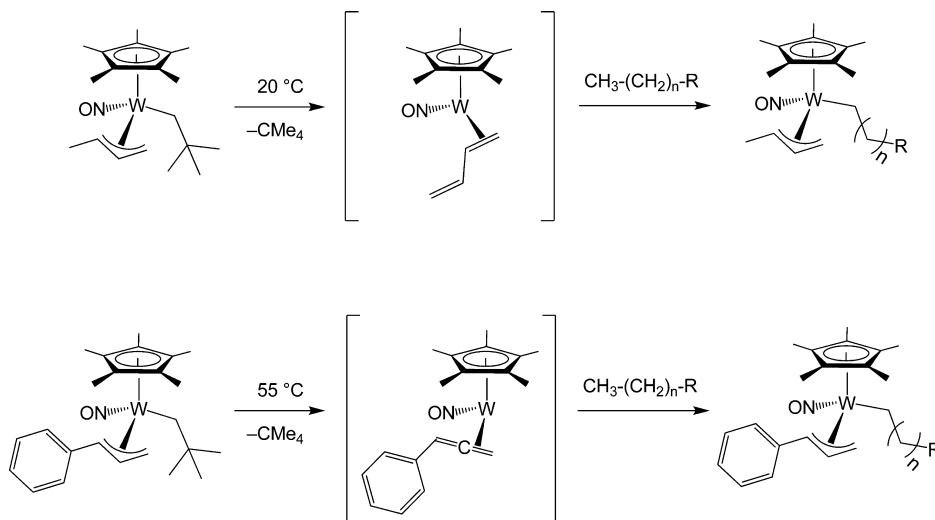
compounds in order to fully understand their chemistry. A portion of this work has been communicated previously.⁷

RESULTS AND DISCUSSION

Reactions of the $\text{Cp}^*\text{W}(\text{NO})(\text{CH}_2\text{CMe}_3)(\eta^3\text{-CH}_2\text{CHCHMe})$ Complexes ($\text{Cp} = \text{Cp}^*, \text{Cp}'$) with Benzene. The first system that we investigated in detail involved the monomethylallyl compounds, since the Cp^* complex was known to form a “complex mixture of organometallic compounds” in benzene.⁵ As a result of our investigations, the various transformations extant in the monomethylallyl systems can be summarized as shown in Scheme 3 with C_6D_6 as the reactive substrate. The conversions depicted in Scheme 3 have been monitored by ^1H NMR spectroscopy, and they have also been effected on a preparative scale with C_6H_6 as the reactant. As illustrated in Scheme 3, the η^2 -diene intermediate complexes A (i.e., either A^* or A')⁸ activate C_6D_6 in the anticipated manner to form the corresponding phenyl derivatives as the two isomers **2a-d₆** and **2b-d₆**. However, **2a-d₆** and **2b-d₆** ultimately convert to the hydrido complexes **3-d₆** and **4-d₆**, respectively, by intramolecular exchange of the newly formed phenyl ligand with a terminal hydrogen atom on the allyl ligand. To the best of our knowledge, this type of isomerization, which is probably mediated by the metal center, is without precedent in the chemical literature.

Our elucidation of the chemistry initiated by these reactants was facilitated by our discovery that replacement of the Cp^* ligand in the monomethylallyl reactant by the less sterically demanding Cp' group results in significantly slower reaction rates.⁷ Thus, as illustrated in Figure 1, the C–H activation of benzene at 26 °C by $\text{Cp}'\text{W}(\text{NO})(\text{CH}_2\text{CMe}_3)(\eta^3\text{-CH}_2\text{CHCHMe})$ (**1'**) affords only the isomeric phenyl complexes **2a'** and **2b'** during the first 24 h.⁹ In contrast, the identical reaction involving **1*** results after 4 h in the production of at least five new organometallic complexes (counting the isomer of **3**, which is not shown in Scheme 3). Crystallization of **2'** from pentane provides crystals that contain both **2a'** and **2b'** in the lattice (Figure 2), but similar treatment of **2*** produces crystals that contain only **2a*** (Figure 3) whose intramolecular dimensions are essentially identical with those of **2a'**. As in other $\text{Cp}^*\text{W}(\text{NO})(\text{alkyl})(\eta^3\text{-allyl})$ complexes,² the allyl ligands of complexes **2** are in endo orientations with the

Scheme 2



Scheme 3

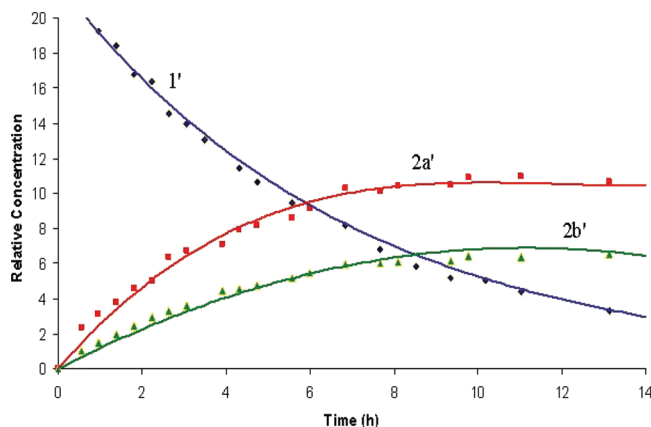
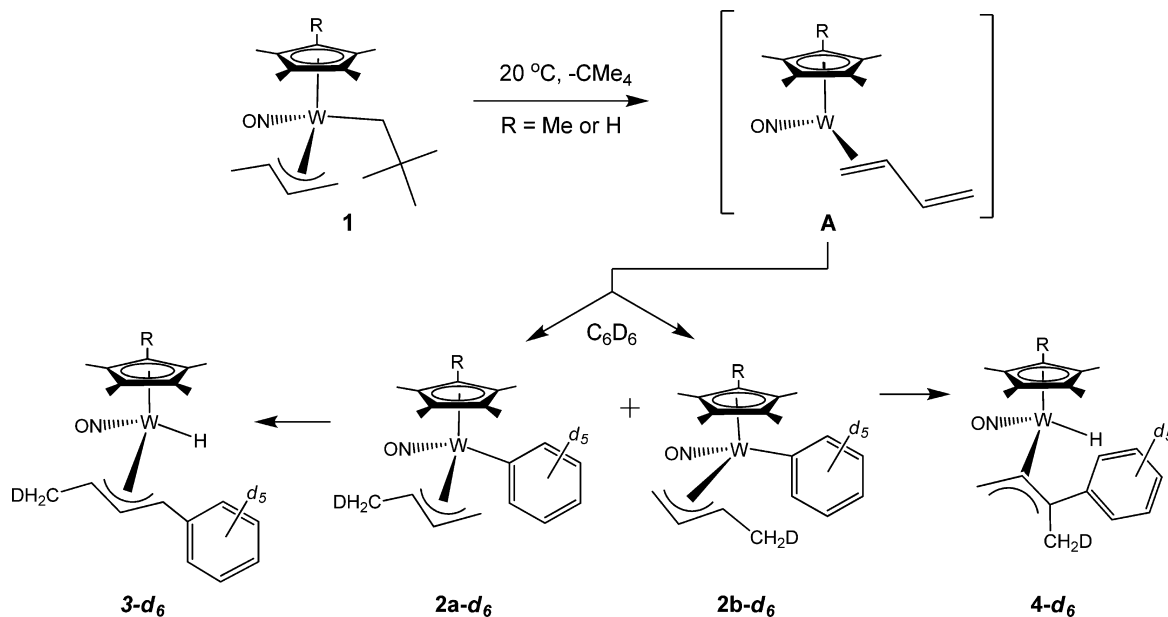


Figure 1. Distribution of organometallic complexes during the C–H activation of benzene by **1'** at 26 °C.

meso protons pointing away from the cyclopentadienyl rings. Furthermore, there is a σ – π distortion of the allyl ligands brought about by the electronic asymmetry at the metal centers.¹⁰ The spectroscopic properties of complexes **2** indicate that they retain their “piano-stool” molecular structures in solution. Interestingly, dissolution of crystals of **2a*** in C_6D_6 immediately results in a solution whose ^1H NMR spectrum exhibits signals attributable to both **2a*** and **2b***, thereby indicating that the two isomers are in rapid equilibrium with each other.

The synthesis of isomeric complexes **3*** (minor) and **4*** (major) is facilitated by warming of the reaction mixture to 45 °C for 24 h. Their molecular structures have been deduced from their diagnostic ^1H and ^{13}C APT NMR spectra, and the structure of **4*** has been confirmed by an X-ray crystallographic analysis (Figure 4). The signals due to the hydride ligands in **3*** and **4*** occur at δ –0.63 ppm ($^1J_{\text{WH}} = 124$ Hz) and –0.05 ($^1J_{\text{WH}} = 127$ Hz), respectively, and the intramolecular metrical parameters of **4*** are similar to those of the other new complexes isolated during this work. Interestingly, the allyl ligand in **4*** is in an exo orientation, probably because of the

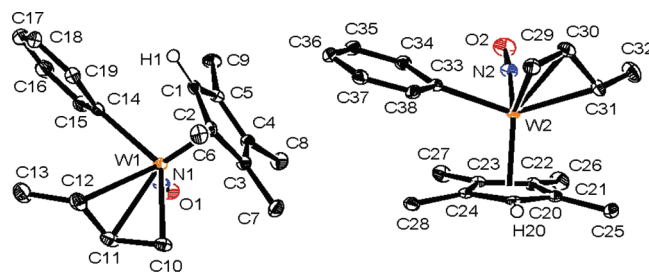


Figure 2. Solid-state molecular structures of **2a'** (right) and **2b'** (left) as they occur in the asymmetric unit with 30% probability thermal ellipsoids shown. Selected interatomic distances (Å) and angles (deg): **2a'**, $\text{W}(2)\text{--C}(29) = 2.360(3)$, $\text{W}(2)\text{--C}(30) = 2.331(3)$, $\text{W}(2)\text{--C}(31) = 2.291(3)$, $\text{W}(1)\text{--C}(33) = 2.214(3)$, $\text{W}(2)\text{--N}(2) = 1.775(3)$, $\text{N}(2)\text{--O}(2) = 1.223(4)$, $\text{C}(29)\text{--C}(30) = 1.378(5)$, $\text{C}(30)\text{--C}(31) = 1.423(5)$, $\text{C}(31)\text{--C}(32) = 1.512(5)$, $\text{C}(29)\text{--C}(30)\text{--C}(31) = 118.2(3)$, $\text{W}(2)\text{--N}(2)\text{--O}(2) = 172.1(3)$; **2b'**, $\text{W}(1)\text{--C}(10) = 2.232(3)$, $\text{W}(1)\text{--C}(11) = 2.357(3)$, $\text{W}(1)\text{--C}(12) = 2.506(3)$, $\text{W}(1)\text{--C}(14) = 2.210(3)$, $\text{W}(1)\text{--N}(1) = 1.773(3)$, $\text{N}(1)\text{--O}(1) = 1.225(4)$, $\text{C}(10)\text{--C}(11) = 1.424(5)$, $\text{C}(11)\text{--C}(12) = 1.367(5)$, $\text{C}(12)\text{--C}(13) = 1.501(5)$, $\text{C}(10)\text{--C}(11)\text{--C}(12) = 119.2(3)$, $\text{C}(11)\text{--C}(12)\text{--C}(13) = 123.1(4)$, $\text{C}(30)\text{--C}(31)\text{--C}(32) = 120.4(3)$, $\text{W}(1)\text{--N}(1)\text{--O}(1) = 169.0(3)$.

two substituents on C(13) (Figure 4).¹¹ The final ^1H NMR spectrum of the mixture of **3*** and **4*** in C_6D_6 also exhibits resonances that may be assigned to the minor coordination isomer of **3***, in which the phenyl substituent on the allyl ligand is situated at the opposite end, adjacent to the nitrosyl group.

Kinetic analyses of the benzene-activation reactions yield pseudo-first-order rate constants (s^{-1}) and Arrhenius activation energies (kJ mol^{-1}) of $(8.5 \pm 0.2) \times 10^{-5}$ and 79.1 ± 1.9 and $(3.6 \pm 0.1) \times 10^{-5}$ and 93.2 ± 6.6 for **1*** and **1'**, respectively. The corresponding Eyring parameters ΔH^\ddagger (kJ mol^{-1}) and ΔS^\ddagger ($\text{J K}^{-1} \text{mol}^{-1}$) are 76.5 ± 1.9 and -66.6 ± 3.0 and 90.6 ± 6.6 and -27.4 ± 3.4 , respectively. The subsequent isomerizations of **2a,b** to the hydrido complexes **3** and **4** also occur more rapidly for the Cp^* complexes. Thus, signals due to **3*** and **4*** begin to appear in the ^1H NMR spectrum of the benzene reaction mixture after 4 h at 26 °C when only 75% of **1*** has

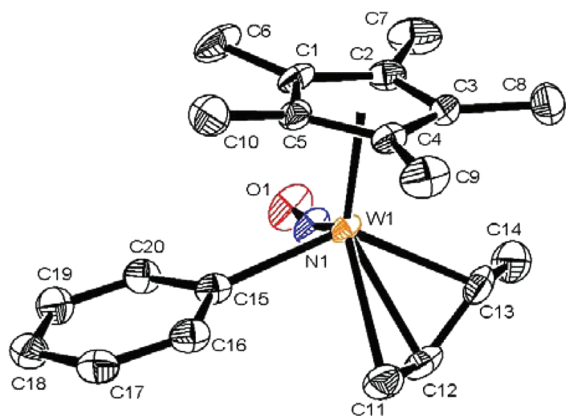


Figure 3. Solid-state molecular structure of **2a*** with 30% probability thermal ellipsoids shown. Selected interatomic distances (Å) and angles (deg): W(1)–C(11) = 2.378(5), W(1)–C(12) = 2.339(5), W(1)–C(13) = 2.277(5), W(1)–C(15) = 2.216(5), W(1)–N(1) = 1.779(4), N(1)–O(1) = 1.220(5), C(11)–C(12) = 1.380(9), C(12)–C(13) = 1.424(9), C(13)–C(14) = 1.476(9), C(11)–C(12)–C(13) = 118.7(5), C(12)–C(13)–C(14) = 120.1(6), W(1)–N(1)–O(1) = 167.8(4).

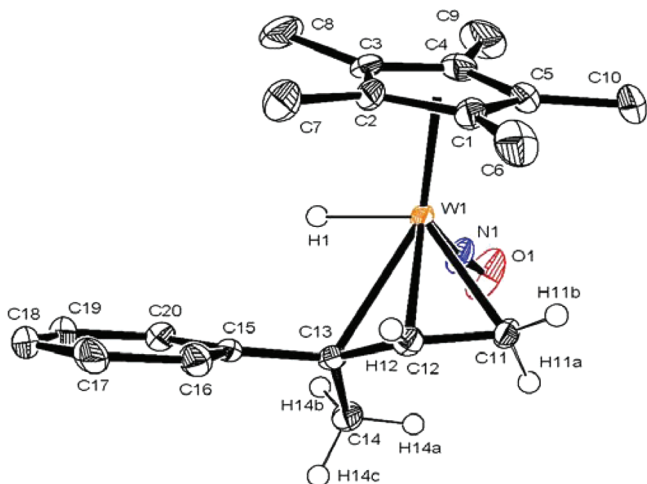


Figure 4. Solid-state molecular structure of **4*** with 30% probability thermal ellipsoids shown. Selected interatomic distances (Å) and angles (deg): W(1)–C(11) = 2.279(3), W(1)–C(12) = 2.279(3), W(1)–C(13) = 2.461(3), W(1)–H(1) = 1.68(4), W(1)–N(1) = 1.774(2), N(1)–O(1) = 1.222(3), C(15)–C(13) = 1.499(4), C(13)–C(12) = 1.400(4), C(12)–C(11) = 1.417(4), C(15)–C(13)–C(12) = 119.4(2), C(13)–C(12)–C(11) = 124.2(3), W(1)–N(1)–O(1) = 175.4(2).

been consumed. In contrast, hydride resonances attributable to **3'** and **4'** only begin to appear after 24 h at 26 °C when 96% of **1'** has reacted. In other words, for the first 24 h the Cp' reaction mixture contains only three organometallic complexes (cf. Figure 1), whereas the Cp* reaction mixture after 4 h under identical conditions contains at least six such compounds: i.e., “a complex mixture”.⁵ Clearly, the isolation of the desired products resulting from the C–H activation of benzene is easiest for the Cp' system.

In general, the C–H activation chemistry exhibited by the monomethylallyl compound Cp'W(NO)(CH₂CMe₃)(η³-CH₂CHCHMe) (**1'**) closely resembles that of its Cp* congener. Specifically, it also initiates sp³ C–H activations of the hydrocarbons exclusively at their terminal carbons and

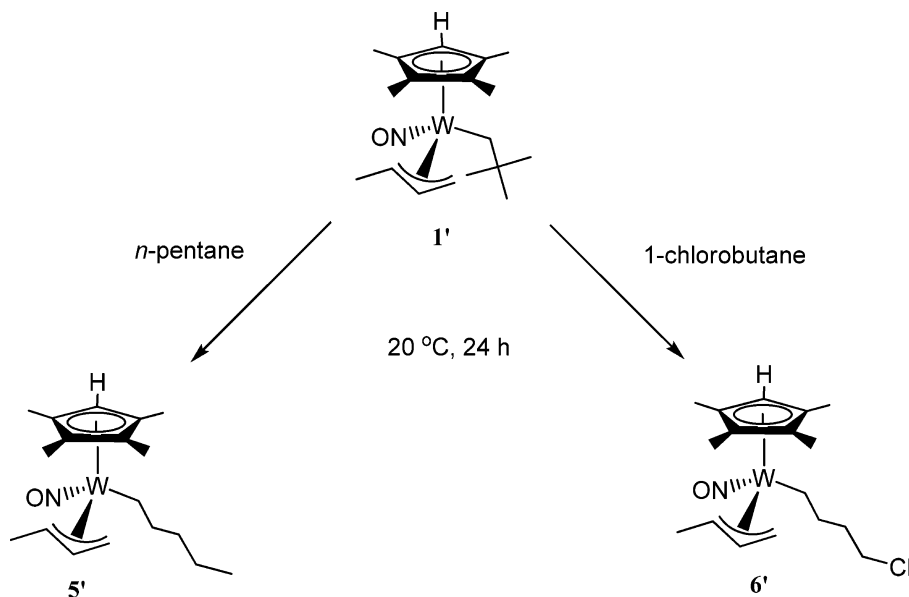
forms Cp'W(NO)(*n*-alkyl)(η³-CH₂CHCHMe) complexes such as **5'** and **6'** shown in Scheme 4, but at a slower rate than the Cp* complex. The practical advantage of the Cp' system is again that the product *n*-alkyl complexes are generally more thermally stable at a particular temperature than are their Cp* analogues.

Reactions of the CpW(NO)(CH₂CMe₃)(η³-CH₂CHCHPh) Complexes (Cp = Cp*, Cp') with Benzene. Given the results obtained with the monomethylallyl complexes **1** as summarized in the preceding section, we decided to ascertain if the situation was equally complex for the related phenylallyl systems. The thermolysis of Cp*W(NO)(CH₂CMe₃)(η³-CH₂CHCHPh) (**7***) in benzene at 75 °C for 1 day leads to the exclusive formation of one new organometallic species (Scheme 5). This pale yellow complex can be purified by chromatography on alumina and crystallized from pentane/Et₂O as needles. An X-ray crystallographic analysis of one of these needles has revealed this compound to be Cp*W(NO)-(H)(η³-PhHCCHCHPh) (**9***), whose solid-state molecular structure is shown in Figure 5. In **9*** the phenyl group resulting from the C–H activation of benzene is attached to the previously unsubstituted end of the phenylallyl ligand, thus converting it into a 1,3-diphenylallyl ligand. A metal–hydride linkage is also present in this compound, as evidenced by a characteristic hydride signal at –0.15 ppm (¹J_{WH} = 124 Hz) in the ¹H NMR spectrum of **9*** in C₆D₆. Labeling experiments with benzene-*d*₆ have confirmed that this transformation does indeed proceed via an intermediate 16e η²-allene complex (Scheme 5).

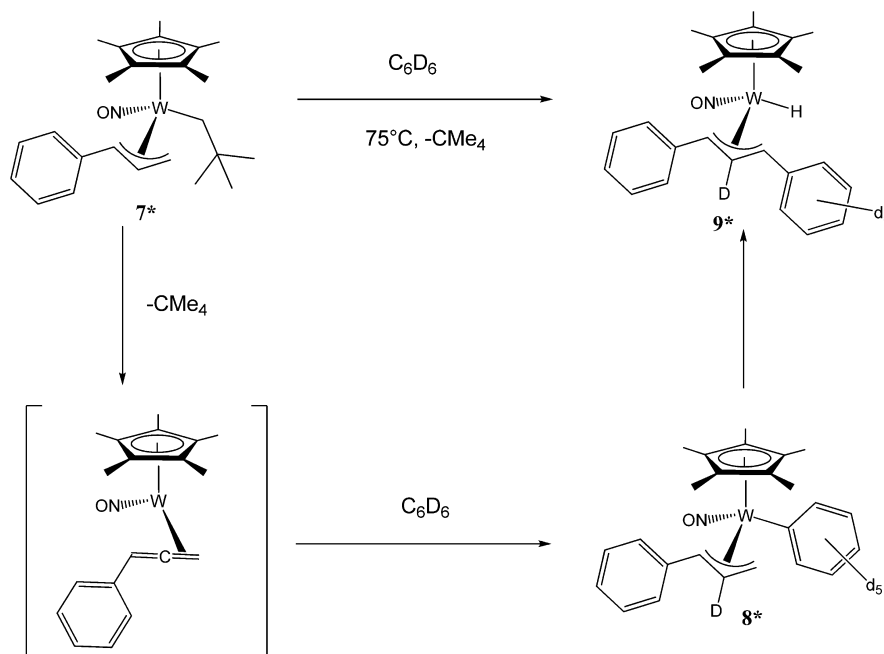
We next decided to synthesize the Cp' analogue of **7*** (i.e., **7'**) and to investigate its thermal behavior in benzene with a view to acquiring additional evidence in support of the mechanism depicted in Scheme 5. Cp'W(NO)(CH₂CMe₃)(η³-CH₂CHCHPh) (**7'**) can be synthesized in moderate yields by utilizing the procedure reported for its Cp* analogue,² and its solid-state molecular structure is shown in Figure 6. The replacement of a methyl group by a hydrogen atom on a cyclopentadienyl ligand is expected to decrease the inductive electronic contribution of the ligand to the tungsten center. Such an effect is manifested by the infrared nitrosyl-stretching frequency of **7'**, which at 1600 cm^{–1} is slightly higher in energy than that exhibited by **7*** at 1588 cm^{–1}. As expected, our investigations of the thermal chemistry of **7'** have revealed that it generally parallels that of **7***, but the transformations proceed at a significantly slower rate.

Thermolysis of **7'** in benzene at 55 °C for 6 days produces the corresponding 1,3-diphenylallyl hydride derivative Cp'W(NO)(H)(η³-PhHCCHCHPh) (**9'**) (Scheme 6). As with complex **1'**, the reaction of **7'** proceeds at a rate slower than that exhibited by the pentamethylcyclopentadienyl analogue **7***. This fact facilitates the isolation of the phenyl derivative Cp'W(NO)(C₆H₅)(η³-CH₂CHCHPh) (**8'**), following thermolysis of **7'** in benzene for 22 h and subsequent purification by column chromatography. The isolation of **8'** supports the mechanism depicted in Scheme 5, in which complex **9*** is formed via the initial C–H activation of benzene, leading to the phenyl derivative **8***, followed by the subsequent aryl–hydrogen isomerization. The rates of conversion of **7'** to **8'** and **8'** to **9'** are again slower than those observed for the analogous transformations of **7*** and **8***. Hence, the slower rates of reaction of the Cp' complexes thus permit them to be used as models for the Cp* systems in order to investigate more fully the mechanistic details of the thermal C–H bond-

Scheme 4



Scheme 5



activation chemistry of various $Cp^*W(NO)(alkyl)(\eta^3\text{-allyl})$ complexes.

Reaction of $Cp^*W(NO)(CH_2CMe_3)(\eta^3\text{-CH}_2\text{CHCHPh})$ with Methylcyclohexane. During our investigations we have discovered that the reactions of $Cp^*W(NO)(CH_2CMe_3)(\eta^3\text{-CH}_2\text{CHCHPh})$ (**7***) with methyl- and ethylcyclohexane provide some insights as to the conversions that occur when multiple products are formed during the C–H activations of alkanes initiated by these systems. We have previously reported that thermolysis of **7*** in methylcyclohexane at 55 °C for 2 days affords a single organometallic complex, namely dark orange $Cp^*W(NO)(CH_2C_6H_{11})(\eta^3\text{-CH}_2\text{CHCHPh})$ (**10***), as well as some unreacted starting material.⁶ We have now discovered that continuing the thermolysis for 4 days in total leads to the

formation of two different organometallic complexes (Scheme 7).

The major organometallic product, $Cp^*W(NO)(\eta^3\text{-C}_7\text{H}_{11})(H)$ (**11***), arises from two additional C–H activations of the methylcyclohexyl ligand, a process accompanied by the loss of the phenylallyl group from the metal's coordination sphere. Complex **11*** has been previously prepared in our laboratories via two routes. It was first made as an isomeric mixture by thermolysis of $Cp^*W(NO)(CH_2CMe_3)_2$ in methylcyclohexane.¹² A similar experiment using $Cp^*W(NO)(CH_2CMe_3)(\eta^3\text{-CH}_2\text{CHCMe}_2)$ afforded the same products, albeit in a slightly different ratio.⁴ The 1H NMR spectrum of the final reaction mixture following the prolonged thermolysis of **7*** clearly exhibits signals diagnostic of **11*** (i.e., $\delta -0.72$ (s, $^1J_{WH} = 123$ Hz, 1H, WH), 1.77 (s, 15H, C_5Me_5)).

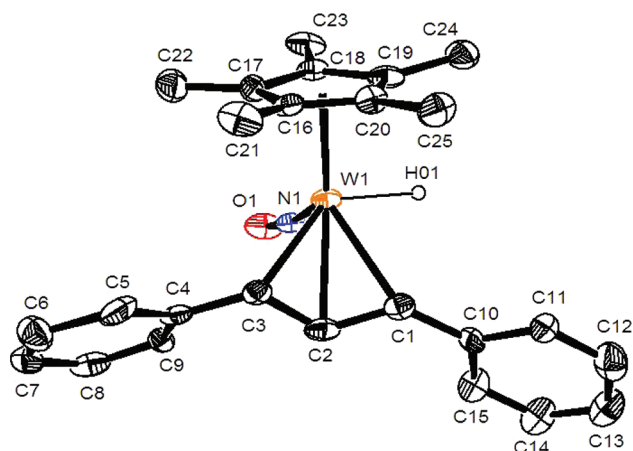


Figure 5. Solid-state molecular structure of one of the independent molecules of $\text{Cp}^*\text{W}(\text{NO})(\text{H})(\eta^3\text{-PhHCCHCHPh})$ (9^*) with 30% probability thermal ellipsoids shown. Selected interatomic distances (Å) and angles (deg): $\text{W}(1)\text{-C}(1) = 2.406(10)$, $\text{W}(1)\text{-C}(2) = 2.302(9)$, $\text{W}(1)\text{-C}(3) = 2.264(9)$, $\text{W}(1)\text{-N}(1) = 1.758(7)$, $\text{N}(1)\text{-O}(1) = 1.226(10)$, $\text{C}(1)\text{-C}(2) = 1.409(15)$, $\text{C}(2)\text{-C}(3) = 1.368(14)$, $\text{C}(3)\text{-C}(4) = 1.471(14)$, $\text{C}(1)\text{-C}(10) = 1.454(14)$, $\text{C}(1)\text{-C}(2)\text{-C}(3) = 120.0(10)$, $\text{C}(2)\text{-C}(3)\text{-C}(4) = 122.3(10)$, $\text{C}(2)\text{-C}(1)\text{-C}(10) = 126.0(10)$, $\text{W}(1)\text{-N}(1)\text{-O}(1) = 169.7(7)$.

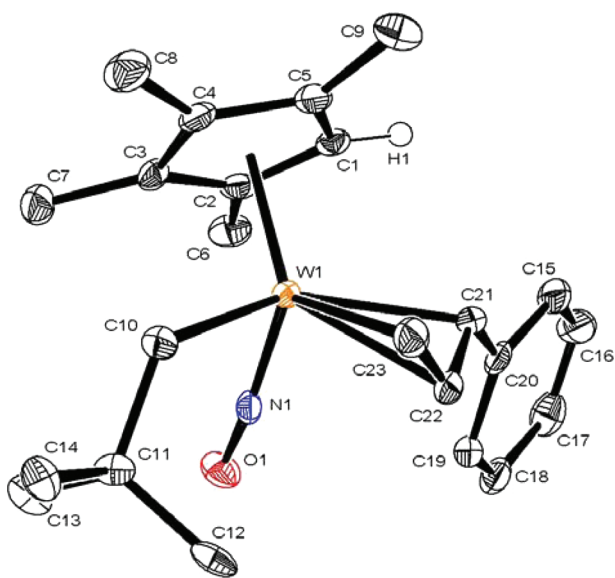


Figure 6. Solid-state molecular structure of 7^* with 30% probability thermal ellipsoids shown. Selected interatomic distances (Å) and angles (deg): $\text{W}(1)\text{-C}(21) = 2.305(5)$, $\text{W}(1)\text{-C}(22) = 2.322(5)$, $\text{W}(1)\text{-C}(23) = 2.375(5)$, $\text{W}(1)\text{-C}(10) = 2.249(6)$, $\text{W}(1)\text{-N}(1) = 1.775(5)$, $\text{N}(1)\text{-O}(1) = 1.218(6)$, $\text{C}(20)\text{-C}(21) = 1.474(8)$, $\text{C}(21)\text{-C}(22) = 1.422(7)$, $\text{C}(22)\text{-C}(23) = 1.378(8)$, $\text{C}(21)\text{-C}(22)\text{-C}(23) = 118.6(5)$, $\text{C}(20)\text{-C}(21)\text{-C}(22) = 125.8(5)$, $\text{W}(1)\text{-C}(10)\text{-C}(11) = 123.6(4)$, $\text{W}(1)\text{-N}(1)\text{-O}(1) = 170.7(4)$.

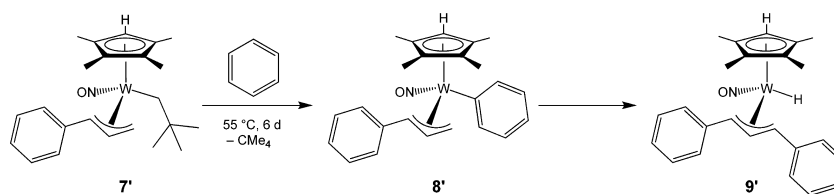
The minor product, $\text{Cp}^*\text{W}(\text{NO})(\text{H})(\eta^3\text{-CH}(\text{CH}_2\text{C}_6\text{H}_{11})\text{-CHCHPh})$ (12^*), has been fully characterized and is an isomer of 10^* that results from the formal exchange of the methylcyclohexyl group at the metal center with a terminal hydrogen atom of the phenylallyl ligand. It thus resembles the isomerizations of the allyl phenyl complexes described in the preceding sections. Consistently, in the ^1H NMR spectrum of 12^* in C_6D_6 the C_5Me_5 singlet at 1.69 ppm integrates as 15:1:1 to the tungsten hydride resonance at -1.10 ppm and the doublet of doublets due to the allyl meso hydrogen at 5.19 ppm. Consistently, the coupling constants for this doublet of doublets are the same as two of those for the doublet of doublets of doublets attributable to the meso hydrogen of the allyl ligand in complex 7^* (Figure 7), thereby confirming that the methylcyclohexyl group is indeed a terminal substituent on the phenylallyl ligand in 12^* .

A plausible mechanism for the rearrangement of 10^* to 12^* is shown in Scheme 8. It begins with 10^* being in its least sterically congested configuration: i.e., the phenyl substituent on the allyl ligand is proximal to the nitrosyl ligand and distal to the methylcyclohexyl ligand. The alkyl ligand can then effect an intramolecular nucleophilic attack on the phenylallyl CH_2 terminus. A hydrogen from the same allyl carbon atom is then abstracted by the tungsten to form the 16-electron intermediate $\text{Cp}^*\text{W}(\text{NO})(\eta^1\text{-H})(\eta^1\text{-CH}(\text{CH}_2\text{C}_6\text{H}_{11})\text{C}(\text{H})=\text{CHPh})$, which rapidly isomerizes to the 18-electron complex 12^* (Scheme 8).

The reaction of $\text{Cp}^*\text{W}(\text{NO})(\text{CH}_2\text{CMe}_3)(\eta^3\text{-CH}_2\text{CHCHPh})$ (7^*) with methylcyclohexane thus first forms the product resulting from the single activation of a terminal methyl sp^3 C–H bond, namely $\text{Cp}^*\text{W}(\text{NO})(\text{CH}_2\text{C}_6\text{H}_{11})(\eta^3\text{-CH}_2\text{CHCHPh})$ (10^*). However, longer reaction times result in the conversion of 10^* to a mixture of the allyl hydrido complexes 11^* and 12^* , the former resulting from two additional C–H activations of the methylcyclohexyl group and the latter being formed by the formal exchange of the methylcyclohexyl group at the metal center with a terminal hydrogen atom of the phenylallyl ligand (Scheme 7).

Reaction of $\text{Cp}^*\text{W}(\text{NO})(\text{CH}_2\text{CMe}_3)(\eta^3\text{-CH}_2\text{CHCHPh})$ with Ethylcyclohexane. The thermolysis of 7^* in ethylcyclohexane initially proceeds in a manner similar to its reaction with methylcyclohexane: namely, a methyl C–H bond of the solvent is selectively activated to produce $\text{Cp}^*\text{W}(\text{NO})(\text{CH}_2\text{CH}_2\text{C}_6\text{H}_{11})(\eta^3\text{-CH}_2\text{CHCHPh})$ (13^*).⁶ Extended thermolysis leads only to the formation of the two isomers of $\text{Cp}^*\text{W}(\text{NO})(\text{H})(\eta^3\text{-C}_8\text{H}_{13})$ (14a^* and 14b^*) resulting from multiple C–H bond activations of ethylcyclohexane (Scheme 9). The isomeric complexes 14a^* and 14b^* have been previously prepared by the thermolysis of $\text{Cp}^*\text{W}(\text{NO})(\text{CH}_2\text{CMe}_3)_2$ in ethylcyclohexane.¹² Consequently, the compounds synthesized during this work were identified by comparing their ^1H NMR spectra to those previously reported. Interestingly, the cyclohexylethyl ligand in complex 13^* does

Scheme 6



Scheme 7

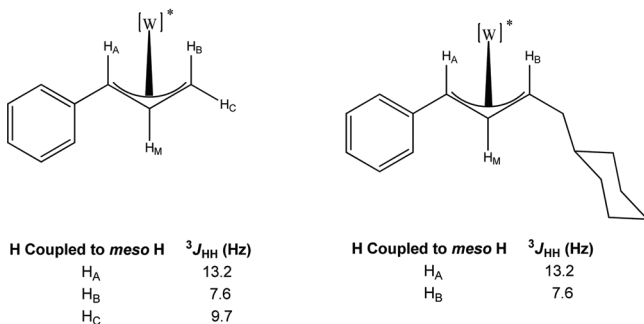
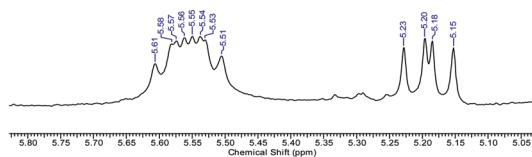
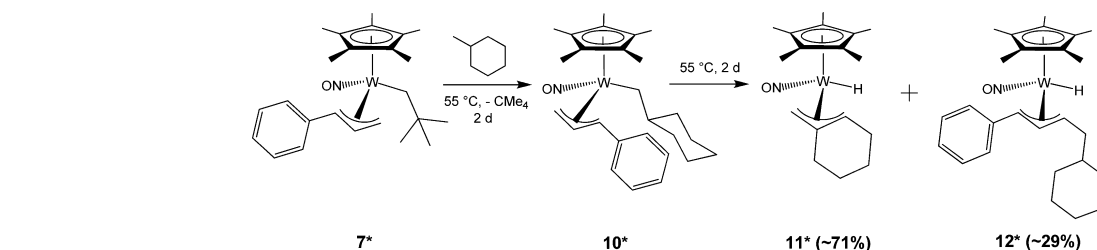
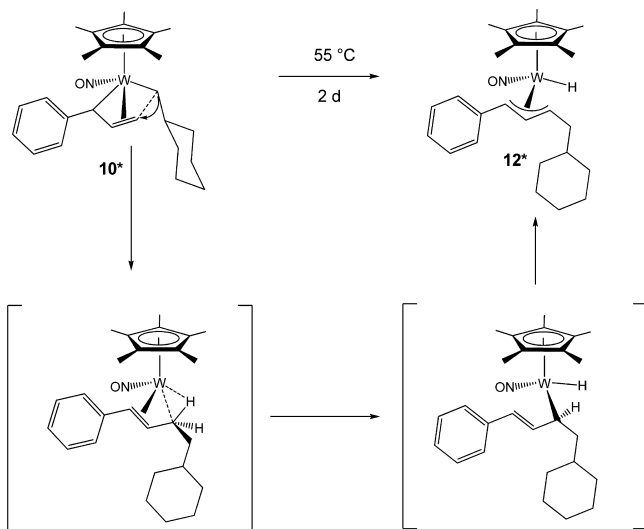


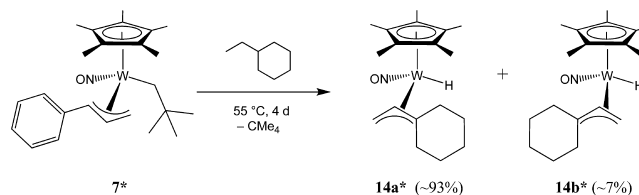
Figure 7. Expansion of the ^1H NMR spectrum (5.83 to 5.03 ppm) of 7^* and 12^* in C_6D_6 displaying the resonances due to the meso CH protons of 7^* (δ 5.56, $^3J_{\text{HH}} = 13.2, 9.7, 7.6$ Hz) and 12^* (δ 5.19, $^3J_{\text{HH}} = 13.2, 9.7$ Hz) and the schematic for meso hydrogen coupling in 7^* (left) and 12^* (right).

Scheme 8



not undergo migration to the phenylallyl ligand as does the cyclohexylmethyl group during the conversion of 10^* into 12^* (Scheme 8). Since complexes 10^* and 13^* exhibit similar IR nitrosyl stretching frequencies, the presence or absence of an alkyl migration event is likely due primarily to steric rather than electronic influences. In complex 10^* the cyclohexyl group is separated from the tungsten center by a single carbon atom, while for the cyclohexylethyl ligand there is a two-carbon

Scheme 9



distance between the cyclohexyl group and the tungsten center. Thus, the cyclohexylmethyl group is more sterically crowded at the metal center in 10^* , and that may well account for its proclivity to effect the alkyl–hydrogen exchange which forms complex 12^* . Consistent with this conclusion is the fact that we have never observed the intramolecular migration of a linear alkyl ligand to the allyl group in any of our systems.

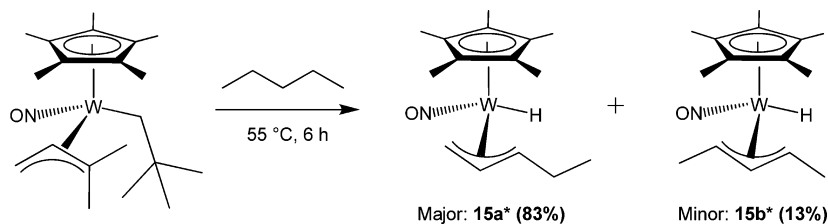
The extrapolation of these results to the C–H activation of linear alkanes by η^2 -allene intermediate complexes (such as $\text{Cp}^*\text{W}(\text{NO})(\eta^2\text{-H}_2\text{C}=\text{C}=\text{CMe}_2)$ generated from the dimethylallyl complex) is straightforward and accounts for why the final reaction mixtures contain a number of hydrido allyl complexes. Specifically, the thermolysis of $\text{Cp}^*\text{W}(\text{NO})(\text{CH}_2\text{CMe}_3)(\eta^3\text{-CH}_2\text{CHCMe}_2)$ in *n*-pentane leads to the formation of isomers of $\text{Cp}^*\text{W}(\text{NO})(\text{H})(\eta^3\text{-C}_5\text{H}_9)$ ($15\text{a}^*, \text{b}^*$), which result from multiple C–H activations of the solvent molecules (Scheme 10).

Role of Electron Densities at the Tungsten Centers. As summarized in Table 1, a correlation exists between the observed thermal chemistry of the various $\text{Cp}^*\text{W}(\text{NO})(\text{R})(\eta^3\text{-allyl})$ (R = alkyl, aryl) complexes and the electron densities at the tungsten centers of these compounds, as indicated by their infrared nitrosyl stretching frequencies.

For instance, $\text{Cp}^*\text{W}(\text{NO})(\text{CH}_2\text{CMe}_3)(\eta^3\text{-CH}_2\text{CHCHMe})$ (**1**) (entry 3) and $\text{Cp}^*\text{W}(\text{NO})(\text{CH}_2\text{CMe}_3)(\eta^3\text{-CH}_2\text{CHCHPh})$ (7^*) (entry 7) have higher nitrosyl stretching frequencies and thus less electron rich tungsten centers. These two complexes initiate the activation of only a single primary sp^3 C–H bond of alkane substrates. In contrast, $\text{Cp}^*\text{W}(\text{NO})(\text{CH}_2\text{CMe}_3)(\eta^3\text{-CH}_2\text{CHCMe}_2)$ (entry 1) has a lower nitrosyl stretch and a more electron rich tungsten center, and this complex facilitates multiple C–H bond activations of alkane substrates. This correlation can also be applied to the complexes resulting from the initial C–H activations. Thus, as demonstrated during this work, subsequent C–H bond activations occur with complexes 10^* and 13^* (entries 11 and 12), which again have more electron rich tungsten centers. Such multiple C–H activations of a substrate occur via intramolecular hydrogen transfer processes mediated by the tungsten centers, and these processes are evidently more facile for the more electron-rich metal centers.

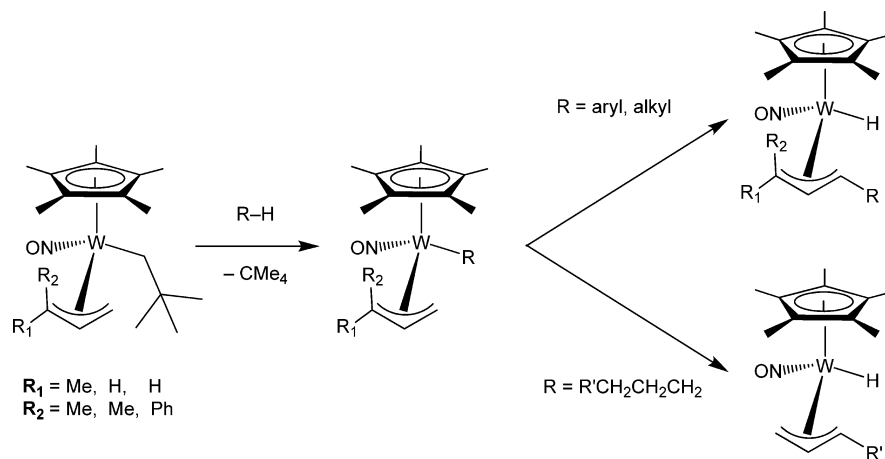
The other transformation that can occur with a $\text{Cp}^*\text{W}(\text{NO})(\text{R})(\eta^3\text{-allyl})$ complex resulting from initial activation of

Scheme 10

**Table 1. Correlation of Nitrosyl Stretching Frequencies of Some CpW(NO)(R)(η^3 -allyl) (R = Alkyl, Aryl) Complexes with Their Reactivities**

entry	complex	ν_{NO} (Nujol, cm^{-1})	multiple alkane C–H activations?	R–allyl H exchange?	ref
1	$\text{Cp}^*\text{W}(\text{NO})(\text{CH}_2\text{CMe}_3)(\eta^3\text{-CH}_2\text{CHCMe}_2)$	1546	yes	no	4
2	$\text{Cp}^*\text{W}(\text{NO})(\text{Ph})(\eta^3\text{-CH}_2\text{CHCMe}_2)$	1562	no	no	4
3	$\text{Cp}^*\text{W}(\text{NO})(\text{CH}_2\text{CMe}_3)(\eta^3\text{-CH}_2\text{CHCHMe})$ (1*)	1594	no	no	5 and this work
4	$\text{Cp}^*\text{W}(\text{NO})(\text{CH}_2\text{CMe}_3)(\eta^3\text{-CH}_2\text{CHCHMe})$ (1')	1595	no	no	this work
5	$\text{Cp}^*\text{W}(\text{NO})(\text{C}_6\text{D}_5)(\eta^3\text{-CH}_2\text{CDCHMe})$ (2*)		no	yes	this work
6	$\text{Cp}^*\text{W}(\text{NO})(\text{C}_6\text{D}_5)(\eta^3\text{-CH}_2\text{CDCHMe})$ (2')		no	yes	this work
7	$\text{Cp}^*\text{W}(\text{NO})(\text{CH}_2\text{CMe}_3)(\eta^3\text{-CH}_2\text{CHCHPh})$ (7*)	1588	no	no	this work
8	$\text{Cp}^*\text{W}(\text{NO})(\text{CH}_2\text{CMe}_3)(\eta^3\text{-CH}_2\text{CHCHPh})$ (7')	1591	no	no	this work
9	$\text{Cp}^*\text{W}(\text{NO})(\text{Ph})(\eta^3\text{-CH}_2\text{CHCHPh})$ (8*)		no	yes	this work
10	$\text{Cp}^*\text{W}(\text{NO})(\text{Ph})(\eta^3\text{-CH}_2\text{CHCHPh})$ (8')	1591	no	yes	this work
11	$\text{Cp}^*\text{W}(\text{NO})(\text{CH}_2\text{C}_6\text{H}_{11})(\eta^3\text{-CH}_2\text{CHCHPh})$ (10*)	1562	yes	yes	6 and this work
12	$\text{Cp}^*\text{W}(\text{NO})(\text{CH}_2\text{CH}_2\text{C}_6\text{H}_{11})(\eta^3\text{-CH}_2\text{CHCHPh})$ (13*)	1562	yes	no	6 and this work

Scheme 11



an R–H bond is most commonly encountered when R–H is benzene, and it involves exchange of the phenyl ligand with a terminal hydrogen atom of the allyl ligand, a typical example being shown in Scheme 3 (vide supra). A plausible mechanism for this isomerization involves intramolecular nucleophilic attack by the phenyl ligand on the CH_2 terminus of the η^3 -allyl group. Such an attack would be favored for a complex having a relatively electrophilic allyl ligand attached to a less electron rich tungsten center. Consistent with this view is the fact that such isomerizations do indeed occur for $\text{Cp}^*\text{W}(\text{NO})\text{-}(\text{R})(\eta^3\text{-allyl})$ complexes having relatively higher nitrosyl stretching frequencies: e.g. entries 5, 6, and 9. Interestingly, the electronic conditions in complexes **10*** and **13*** (entries 11 and 12) are such that subsequent multiple C–H activations occur in both complexes, yet only complex **10*** also undergoes an alkyl hydrogen isomerization process. This observation suggests that while an electronic influence is important for multiple C–H activation processes, sterics still play a significant

role in the alkyl/aryl isomerizations. Apparently the decreased steric congestion at the tungsten center of **13*** as compared to **10*** means that the isomerization pathway is sufficiently slowed with respect to the multiple C–H activation route such that no cyclohexylethyl analogue of **12*** is formed.

Epilogue. In order to be of use in a practical sense, the C–H activations initiated by these $\text{Cp}^*\text{W}(\text{NO})(\text{CH}_2\text{CMe}_3)(\eta^3\text{-allyl})$ complexes ($\text{Cp} = \text{Cp}^*, \text{Cp}'$) must be selective and afford single organometallic products in good yields. The results of the investigations reported in this article have established that single activations of arenes such as benzene are best effected with the dimethylallyl complex $\text{Cp}^*\text{W}(\text{NO})(\text{CH}_2\text{CMe}_3)(\eta^3\text{-CH}_2\text{CHCMe}_2)$ at 50 °C, whereas the specific activation of terminal sp^3 C–H bonds of alkanes are best effected with the monomethylallyl complex $\text{Cp}^*\text{W}(\text{NO})(\text{CH}_2\text{CMe}_3)(\eta^3\text{-CH}_2\text{CHCHMe})$ (**1***) at ambient temperatures or with the phenylallyl complex $\text{Cp}^*\text{W}(\text{NO})(\text{CH}_2\text{CMe}_3)(\eta^3\text{-CH}_2\text{CHCHPh})$ (**7***) at 55 °C. The Cp' analogues of the

Cp* allyl complexes display similar C–H activation chemistry, but at a slower rate, and the resulting Cp*W(NO)(η^1 -hydrocarbyl)(η^3 -allyl) complexes exhibit greater thermal stability at a particular temperature than do their Cp* counterparts. These desirable C–H activating characteristics correlate with the tungsten centers in the product compounds being somewhat electron poor and exhibiting relatively higher nitrosyl-stretching frequencies in their infrared spectra. Reactions of the three Cp*W(NO)(CH₂CMe₃)(η^3 -allyl) complexes at temperatures higher than those specified above or with other hydrocarbon substrates begin to afford other products, as summarized in Scheme 11. These other compounds are (a) Cp*W(NO)(H)[η^3 -(hydrocarbyl)allyl] complexes that are isomers of the CpW(NO)(η^1 -hydrocarbyl)(η^3 -allyl) compounds resulting from an intramolecular hydrocarbyl/allylH exchange and (b) Cp*W(NO)(H)[η^3 -hydrocarbyl] species that result from three successive C–H activations of the hydrocarbon substrate and loss of the original allyl ligand. Our current investigations are centered on releasing the η^1 -hydrocarbyl ligands formed by the desired single C–H activation processes from the tungsten's coordination sphere in an appropriately functionalized manner, and the results of these studies will be reported in due course.

EXPERIMENTAL SECTION

General Methods. All reactions and subsequent manipulations involving organometallic reagents were performed under anhydrous and anaerobic conditions under either high vacuum or an inert atmosphere of prepurified dinitrogen or argon. Purification of inert gases was achieved by passing them first through a column containing MnO and then a column of activated 4 Å molecular sieves. Conventional glovebox and Schlenk techniques were utilized throughout. The gloveboxes utilized were Innovative Technologies LabMaster 100 and MS-130 BG dual-station models equipped with freezers maintained at –30 °C. All glassware was heated in an oven to 275 °C to remove any moisture and then cooled to room temperature under vacuum. Most reactions were performed in thick-walled glass vessels possessing Kontes greaseless stopcocks and side arm inlets for vacuum-line attachment. Small-scale reactions and NMR spectroscopic analyses were conducted in J. Young NMR tubes equipped with Kontes greaseless stopcocks. All solvents were dried with appropriate drying agents under a dinitrogen atmosphere and were distilled prior to use, or they were transferred directly under vacuum from the appropriate drying agent. Hydrocarbon solvents, pentane, diethyl ether (Et₂O), benzene, and benzene-*d*₆ were dried over sodium/benzophenone ketyl and freshly distilled prior to use. The syntheses of (CH₂CHCHPh)MgCl and (Me₃CCH₂)MgCl from cinnamyl chloride and neopentyl chloride, respectively, and magnesium (Strem) were performed in a manner similar to that described previously for the preparation of other allyl- and alkylmagnesium reagents, and they were transformed into the corresponding bis(allyl)- and bis(alkyl)magnesium reagents in the usual manner.¹³ Cp*W(NO)(CH₂CMe₃)(η^3 -CH₂CHCHMe) (1*) was prepared according to the published procedure,⁵ and tetramethylcyclopentadiene was obtained from the Boulder Scientific Co. All other chemicals were ordered from commercial suppliers and were used as received. The progress of most reactions was monitored by NMR spectroscopy, but the isolated yields of all new complexes have not been optimized.

Unless otherwise specified, all IR samples were prepared as Nujol mulls sandwiched between NaCl plates, and their spectra were recorded on a Thermo Nicolet Model 4700 FT-IR spectrometer. NMR spectra were recorded at room temperature on Bruker AV-300 or AV-400 instruments, and all chemical shifts and coupling constants are reported in ppm and in Hz, respectively. ¹H NMR spectra were referenced to the residual protio isotopomer present in C₆D₆ (7.16 ppm), and ¹³C NMR spectra were referenced to the natural-abundance carbon signal of C₆D₆ (128.39 ppm). When necessary, ¹H–¹H COSY,

¹H–¹³C HSQC, ¹H–¹³C HMBC, and ¹³C APT experiments were carried out to correlate and assign ¹H and ¹³C NMR signals. Low-resolution mass spectra (EI, 70 eV) were recorded by the staff of the UBC mass spectrometry facility using a Kratos MS-50 spectrometer. Elemental analyses were performed by Mr. David Wong of the UBC microanalytical facility.

Synthesis of Cp*W(NO)(CO)₂. In a glovebox, a three-neck round-bottom flask was charged with NaCp* (4.00 g, 27.7 mmol) and was attached to a Schlenk line. To the flask was added THF (160 mL) by cannulation under a flow of argon. W(CO)₆ (9.90 g, 28.1 mmol) was then added to the orange-yellow solution. The reaction mixture was refluxed at 60 °C for a period of 3 days, during which time the solution became dark brown-black. A 250 mL Schlenk tube was then charged with Diazald (5.57 g, 26.0 mmol) and THF (75 mL), and the resulting solution was added dropwise by cannula into the three-neck round-bottom flask. The final mixture was stirred at ambient temperature for 1 h, whereupon it was transferred into a sublimation flask, and the solvent was removed in vacuo. Sublimation of the residue at 80 °C under dynamic vacuum resulted in the deposition of orange-red crystals of Cp*W(NO)(CO)₂ onto the cold finger (9.61 g, 89% yield).

Characterization Data for Cp*W(NO)(CO)₂. IR (cm⁻¹): 1660 (s, ν_{NO}), 1917 (s, ν_{CO}), 1996 (s, ν_{CO}). ¹H NMR (300 MHz, C₆D₆): δ 1.60 (s, 6H, Cp*Me), 1.67 (s, 6H, Cp*Me), 4.59 (s, 1H, Cp*H). ¹³C APT NMR (100 MHz, C₆D₆): δ 10.5, 12.4 (C₅Me₄H), 88.6 (Cp*CH), 106.8 (Cp*Me), 191.5, 222.8 (CO). Anal. Calcd for C₁₁H₁₃NO₃W: C, 33.78; H, 3.35; N, 3.58. Found: C, 33.58; H, 3.27; N, 3.42.

Synthesis of Cp*W(NO)Cl₂. In a glovebox a Schlenk tube was charged with PCl₅ (2.348 g, 11.28 mmol) and a magnetic stir bar. Under a flow of N₂, Cp*W(NO)(CO)₂ (4.439 g, 11.29 mmol) was added to the Schlenk tube. The mixture was cooled to –196 °C with a liquid N₂ bath, and Et₂O (ca. 100 mL) was slowly cannulated on top of the solids. The initially orange contents were warmed to room temperature while being stirred, and after 30 min at 20 °C a dark blue-green solution had formed. The solvent was removed from the final mixture in vacuo to obtain a dark blue-green crystalline solid. The solid was washed twice with pentane (ca. 20 mL) to obtain Cp*W(NO)Cl₂ (3.40 g, 74% yield).

Characterization Data for Cp*W(NO)Cl₂. IR (cm⁻¹): 1615 (s, ν_{NO}). ¹H NMR (300 MHz, C₆D₆): δ 1.42 (s, 6H, Cp*Me), 1.69 (s, 6H, Cp*Me), 4.59 (s, 1H, Cp*H). ¹³C APT NMR (100 MHz, C₆D₆): δ 10.3, 12.1 (C₅Me₄H), 102.1 (Cp*CH), 119.5, 121.7 (Cp*Me). MS (LREI, *m/z*, probe temperature 150 °C): 407 [M⁺, ¹⁸⁴W]. HRMS-EI (*m/z*): [M⁺] calcd for ¹⁸²WC₉H₁₃NO³⁵Cl₂, 402.98564, found 402.98587.

Synthesis of Cp*W(NO)(CH₂CMe₃)(η^3 -CH₂CHCHMe) (1'). A Schlenk tube (ca. 250 mL) was charged with a magnetic stir bar, Cp*W(NO)Cl₂ (3.59 g, 8.84 mmol), and Mg(CH₂CMe₃)₂·x(dioxane) (titer 126 g/mol of R, 1.10 g, 8.70 mmol of R). The Schlenk tube and its contents were then cooled to –196 °C with a liquid N₂ bath, and THF (90 mL) was cannulated dropwise into the Schlenk tube. The reaction mixture was warmed to room temperature and was stirred for 1 h to obtain a purple solution of Cp*W(NO)(CH₂CMe₃)Cl. The THF was then removed in vacuo, and the purple residue was extracted with Et₂O until the extracts were colorless (3 × 25 mL). The combined extracts were cooled to –60 °C with a dry ice/acetone bath. In the glovebox a separate Schlenk tube was charged with a magnetic stir bar and Mg(CH₂CHCHMe)₂·x(dioxane) (titer 121 g/mol of R, 1.05 g, 8.70 mmol of R). The Schlenk tube and its contents were then cooled in a liquid N₂ bath. The purple Cp*W(NO)(CH₂CMe₃)Cl solution was added dropwise via a cannula to the magnesium reagent at a rate slow enough to allow the added solution to freeze upon contact. The frozen mixture was transferred to a dry ice/acetone bath and was stirred for 45 min after it had melted. The reaction mixture gradually turned brown with the concomitant formation of a brown suspension. The dry ice/acetone bath was removed, and the Et₂O was evaporated under reduced pressure. The remaining residue was extracted with pentane (4 × 25 mL), and the extracts were transferred to the top of an alumina (I) column (2 × 8 cm) made up in pentane and supported on a medium-porosity frit. The column was eluted with 4/1 pentane/Et₂O, and the yellow band that developed was eluted and collected. The eluate was taken to dryness in vacuo, and the residue

was recrystallized from 4/1 pentane/Et₂O at -30 °C to obtain **1'** as orange-yellow crystalline blocks (1.9 g, 47% yield).

Characterization Data for 1'. IR (cm⁻¹): 1595 (s, ν_{NO}). ¹H NMR (400 MHz, C₆D₆): selected signals δ 1.02 (m, 1H, allyl CHCH₃), 1.06 (d, ³J_{HH} = 13.8, 1H, CH₂Me₃), 1.32 (obscured, 1H, allyl CH₂), 1.34 (s, 9H, CH₂Me₃), 1.39 (s, 3H, Cp'Me), 1.40 (s, 3H, Cp'Me), 1.55 (s, 3H, Cp'Me), 1.67 (obscured, 1H, CH₂Me₃), 1.69 (s, 3H, Cp'Me), 1.90 (d, ³J_{HH} = 5.5, 3H, allyl CH₃), 3.61 (d, ³J_{HH} = 6.3, 1H, allyl CH₂), 4.47 (s, 1H, Cp'H), 4.97 (ddd, ³J_{HH} = 14.1, 9.0, 6.3, 1H, allyl CH). ¹³C APT NMR (100 MHz, C₆D₆) δ 9.6, 10.0, 11.3, 11.4 (Cp' Me), 17.4 (allyl CH₃), 26.9 (CH₂Me₃), 35.0 (CH₂Me₃), 51.9 (allyl CH), 73.2 (allyl CH₂), 101.0 (Cp' CH), 104.8, 106.0, 107.0, 111.1 (Cp' CMe), 114.5 (allyl CH). MS (LREI, *m/z*, probe temperature 100 °C) 461 [M⁺]; HRMS-EI (*m/z*): [M⁺] calcd for ¹⁸⁶WC₁₈H₃₁NO 463.19535, found 463.19494. Anal. Calcd for C₁₈H₃₁NO: C, 46.87; H, 6.77; N, 3.04. Found: C, 45.47; H, 6.54; N, 2.84. Elemental analysis for carbon content was consistently lower than the calculated value. This may be due to incomplete combustion of the solid.

Preparation of Cp*W(NO)(Ph)(η³-MeCCHCH₂) (2a',b'). A 4 dram vial was charged with a sample of **1'** (46 mg, 0.099 mmol) and freshly distilled benzene (5 mL). The reaction mixture was allowed to sit undisturbed at room temperature for a period of 48 h, during which time the initially orange solution turned dark brown. The solvent was then removed from the final reaction mixture in vacuo, the resulting oily brown residue was redissolved in a minimum of 3/1 pentane/Et₂O, and the solution was chromatographed on an alumina column (1 × 4 cm) using a 2/1 pentane/Et₂O mixture as the eluent. The yellow band that developed was eluted and collected, and the solvent was removed from the eluate in vacuo to obtain a yellow oil. Crystals containing both **2a'** and **2b'** (24 mg, 51% yield) were grown by dissolving the yellow oil in a minimal amount of pentane and storing the solution at -30 °C.

IR (C₆D₆, cm⁻¹): 1590 (s, ν_{NO}). MS (LREI, probe temp 100 °C, *m/z*): 467 [M⁺]. Anal. Calcd for C₁₉H₂₃NO: C, 48.84; H, 5.39; N, 3.00. Found: C, 48.53; H, 5.36; N, 2.98.

NMR Data for 2a'. ¹H NMR (300 MHz, C₆D₆): selected signals δ 1.88 (d, ³J_{HH} = 5.5, 3H, allyl Me), 3.50 (d, ³J_{HH} = 7.0, 1H, allyl CH₂), 4.85 (s, 1H, Cp'H), 5.06 (m, 1H, allyl CH). ¹³C APT NMR (75 MHz, C₆D₆): δ 10.6, 9.7, 9.4, 9.2 (C₃Me₃H), 16.9 (allyl Me), 56.1 (allyl CHMe), 73.5 (allyl CH₂), 114.1 (allyl CH), 123.6 (aryl C), 127.3 (aryl C), 143.7 (aryl C), 155.2 (ipso C).

NMR Data for 2b'. ¹H NMR (400 MHz, C₆D₆): δ 0.53 (d, 1H, allyl CH₂), 1.02 (d, ³J_{HH} = 5.5, 3H, allyl Me), 1.66 (m, 1H, allyl CHMe), 3.26 (d, ³J_{HH} = 7.0, 1H, allyl CH₂), 4.65 (s, 1H, Cp'H), 5.06 (m, 1H, allyl CH). ¹³C APT NMR (75 MHz, C₆D₆): δ 11.7, 11.2, 11.1, 10.9 (C₂Me₂H), 17.3 (allyl Me), 42.1 (allyl CH₂), 93.4 (allyl CHMe), 111.6 (allyl CH), 123.2 (aryl C), 128.4 (aryl C), 142.7 (aryl C), 161.8 (ipso C).

Preparation of Cp*W(NO)(Ph)(η³-CH₂CHCHMe) (2a*,b*). A sample of **1*** (88 mg, 0.185 mmol) was transferred into a 4 dram vial and dissolved in C₆H₆ (ca. 2 mL) to obtain an orange solution. The reaction mixture was left at room temperature for 24 h, during which time it turned brown. The solvent was removed in vacuo, the resulting oil was dissolved in pentane, and the solution was transferred to the top of an alumina column (0.5 × 5 cm). A yellow band was eluted from the column with a 3/1 pentane/Et₂O mixture to obtain a dark yellow eluate. Removal of solvent from the eluate under reduced pressure afforded a yellow solid (69 mg, 77% yield). A ¹H NMR spectrum of the solid revealed the presence of compounds **2a***, **2b***, **3***, and **4***. Slow recrystallization of the solid from pentane at -30 °C afforded large orange crystals consisting of only compound **2a***.

Characterization Data for 2a*. IR (cm⁻¹): 1604 (s, ν_{NO}). ¹H NMR (400 MHz, C₆D₆): δ 1.24 (m, 1H, allyl CHMe), 1.45 (s, 15H, C₃Me₃), 1.88 (d, ³J_{HH} = 5.9, 3H, allyl Me), 2.01 (d, ³J_{HH} = 13.7, 1H, allyl CH₂), 3.58 (d, ³J_{HH} = 7.4, 1H, allyl CH₂), 5.08 (ddd, ³J_{HH} = 13.7, 9.8, 7.4, 1H, allyl CH), 7.11 (m, 2H, aryl H), 7.21 (m, 2H, aryl H), 7.74 (m, 1H, aryl H). ¹³C APT NMR (100 MHz, C₆D₆): δ 10.3 (C₃Me₃), 17.3 (allyl Me), 57.7 (allyl CHMe), 75.6 (allyl CH₂), 107.9 (C₃Me₃), 115.3 (allyl CH), 124.3 (aryl C), 127.6 (aryl C), 144.2 (aryl C), 158.1 (ipso C). MS (LREI, *m/z*, probe temperature 150 °C): 481

[M⁺, ¹⁸⁴W]. Anal. Calcd for C₂₀H₂₇NO: C, 49.91; H, 5.65; N, 2.91. Found: C, 49.16; H, 5.60; N, 2.90.

NMR Data for 2b*. ¹H NMR (400 MHz, C₆D₆): δ 0.53 (d, ³J_{HH} = 9.4, 1H, allyl CH₂), 1.12 (d, ³J_{HH} = 6.3, 3H, allyl Me), 1.66 (m, 1H, allyl CHMe), 1.43 (s, 15H, C₃Me₃), 2.38 (d, ³J_{HH} = 6.7, 1H, allyl CH₂), 5.17 (ddd, ³J_{HH} = 13.3, 9.4, 6.7, 1H, allyl CH), 7.09 (m, 2H, aryl H), 7.23 (m, 2H, aryl H), 7.73 (m, 1H, aryl H). ¹³C APT NMR (100 MHz, C₆D₆): δ 10.6 (C₃Me₃), 18.0 (allyl Me), 44.2 (allyl CH₂), 93.9 (allyl CHMe), 107.8 (C₃Me₃), 113.2 (allyl CH), 126.1 (aryl C), 129.6 (aryl C), 143.6 (aryl C), 164.8 (ipso C).

Spectroscopic Detection of Cp*W(NO)(H)(η³-CH(Me)-CHCHPh) (3') and Cp*W(NO)(H)(η³-CH₂CHC(Me)Ph) (4'). Complexes **3'** and **4'** were generated in situ by the thermolysis of **1'** (46 mg, 0.099 mmol) in C₆D₆ at 35 °C for 36 h in a J. Young NMR tube. The ¹H NMR spectrum of the final mixture exhibited signals due to hydride ligands at δ -0.56 (¹J_{WH} = 124 Hz) and 0.02 (¹J_{WH} = 127 Hz) that can be assigned to **3'** and **4'**, respectively, by analogy to **3*** and **4*** (vide infra).

Preparation of Cp*W(NO)(H)(η³-CH(Me)CHCHPh) (3*) and Cp*W(NO)(H)(η³-CH₂CHC(Me)Ph) (4*). Complexes **3*** and **4*** were prepared by the thermolysis of **1*** (121 mg, 0.255 mmol) in C₆H₆ (4 mL) at 45 °C for 24 h. The solvent was removed from the final reaction mixture in vacuo to obtain an oily residue that was transferred to the top of an alumina column (0.5 × 6 cm) made up in pentane. A dark yellow band was eluted from the column with a 5/1 pentane/Et₂O mixture to obtain a yellow eluate. The solvents were removed from the eluate under vacuum, the resulting residue was dissolved in a minimal amount of pentane, and the solution was maintained at -30 °C for 2 h to induce the deposition of a yellow solid that contained **3*** and **4*** in a 1/3 ratio (80 mg, 65% yield). Yellow hedgehog-like crystals of **4*** were obtained by recrystallization of this solid from pentane at -30 °C over 3 days.

Characterization Data for 4*. IR (cm⁻¹): 1588 (s, ν_{NO}). ¹H NMR (400 MHz, C₆D₆): δ -0.05 (s, ¹J_{WH} = 127, 1H, WH), 1.59 (s, 15H, C₃Me₃), 2.17 (s, 3H, allyl Me), 2.50 (d, ³J_{HH} = 7.8, 1H, allyl CH₂), 2.82 (d, ³J_{HH} = 13.3, 1H, allyl CH₂), 3.50 (dd, ³J_{HH} = 13.3, 7.8, 1H, allyl CH), 7.01 (m, 2H, aryl H), 7.12 (m, 2H, aryl H), 7.49 (m, 1H, aryl H). ¹³C APT NMR (100 MHz, C₆D₆): δ 10.7 (C₃Me₃), 24.4 (allyl Me), 42.7 (allyl CH₂), 94.7 (allyl CH), 98.2 (allyl C), 104.6 (C₃Me₃), 126.7 (aryl C), 128.7 (aryl C), 129.0 (aryl C), 146.9 (ipso C). MS (LREI, *m/z*, probe temperature 150 °C): 481 [M⁺, ¹⁸⁴W]. Anal. Calcd for C₂₀H₂₇NO: C, 49.91; H, 5.65; N, 2.91. Found: C, 49.05; H, 5.54; N, 2.94.

Selected Signals Attributable to 3*. ¹H NMR (400 MHz, C₆D₆): δ -0.63 (s, ¹J_{WH} = 124, 1H, WH), 1.69 (s, 15H, C₃Me₃), 5.22 (dd, ³J_{HH} = 12.9, 9.4, 1H, allyl CH). ¹³C APT NMR (100 MHz, C₆D₆): δ 10.9 (C₃Me₃), 105.1 (C₃Me₃), 106.1 (allyl CH).

Monitoring the Conversions of 1 to 2a,b. Complex **1** (either **1'** (40 mg, 0.087 mmol) or **1*** (50 mg, 0.105 mmol)) was dissolved in C₆D₆ (0.8 mL) to obtain a yellow-orange solution that was then transferred into a J. Young NMR tube. The ¹H NMR spectrum of the solution was recorded periodically, and the area under the doublet at δ 3.61 (d, 1H, allyl CH₂) for **1'** and the meso peak at δ 4.97 (ddd, 1H, allyl CH) of **1*** was integrated against the signal at 7.16 ppm corresponding to the residual protio isotopomer present in C₆D₆, which was referenced to 10. These NMR monitoring experiments were performed at approximately 10 °C intervals ranging from 25 to 55 °C for each complex and were continued over a period of 24 h at each temperature in order to determine the rate constant, *k*, at that temperature.

Preparation of Cp*W(NO)(CH₂(CH₂)₃CH₃)(η³-CH₂CHCHMe) (5'). In a glovebox, a sample of **1'** (73 mg, 0.158 mmol) was dissolved in *n*-pentane (6 mL) in a 4 dram vial. The mixture was allowed to sit undisturbed for 24 h at room temperature, after which time the solvent was removed in vacuo. The resulting orange-brown residue was redissolved in pentane (10 mL) and chromatographed on an alumina (I) column (1 × 4 cm) using pentane as the eluent. The yellow band that developed was collected, and the solvent was removed from the eluate in vacuo. The yellow residue was recrystallized from pentane/

Et₂O (2/1) to obtain yellow hedgehog-like crystals of **5'** (55 mg, 75% yield).

Characterization Data for 5'. IR (cm⁻¹): 1600 (s, ν_{NO}). ¹H NMR (300 MHz, C₆D₆): δ 1.05 (m, 1H, allyl CHCH₃), 1.33 (s, 3H, Pentyl CH₃) 1.43, 1.50, 1.60, 1.61 (s, 3H, Cp*Me₄) 1.95 (d, ³J_{HH} = 5.6, 3H, allyl CH₃), 3.14 (d, ³J_{HH} = 7.0, 1H, allyl CH₂), 4.51 (s, 1H, Cp*CH), 4.89 (ddd, ³J_{HH} = 13.7, 9.4, 7.0, 1H, allyl CH). ¹³C APT NMR (75 MHz, C₆D₆): δ 10.08, 11.73 (C₅Me₄H), 15.5 (pentyl CH₃), 18.6 (allyl CH₃) 14.8, 23.8, 35.1, 40.8 (pentyl CH₂), 53.8 (allyl CHCH₃), 73.7 (allyl CH₂), 99.6 (C₅Me₄H), 105.6, 106.6, 107.1, 108.2 (Cp*Me₄), 110.7 (allyl CH). MS (LREI, probe temp 100 °C, m/z): 461 [M⁺]. Anal. Calcd for C₁₈H₃₁NO: C, 46.87; H, 6.77; N, 3.04. Found: C, 46.90; H, 6.56; N, 3.12.

Synthesis of Cp*W(NO)(CH₂(CH₂)₂CH₂Cl)(η³-MeCHCHCH₂) (6'). In a glovebox, complex **1'** (74 mg, 0.160 mmol) was dissolved in 1-chlorobutane (3 mL) in a 4 dram vial. The mixture was allowed to sit undisturbed for 24 h at room temperature, after which time the solvent was removed in vacuo. The resulting orange-brown residue was redissolved in pentane (9 mL), and the solution was chromatographed on an alumina (I) column (1 × 4 cm) using 4/1 pentane/Et₂O (20 mL) as the eluent. The yellow band that eluted was collected, and the solvent was removed from the eluate in vacuo. Yellow rod-shaped crystals of **6'** (20 mg, 26% yield) were obtained by recrystallizing the yellow residue from a minimal amount of pentane (2 mL) at -30 °C.

Characterization Data for 6'. IR (cm⁻¹): 1601 (s, ν_{NO}). ¹H NMR (300 MHz, C₆D₆): δ 1.05 (m, 1H, allyl CHCH₃) 1.39, 1.46, 1.56, 1.58 (s, 3H, Cp*Me₄) 1.91 (d, ³J_{HH} = 5.9, 3H, allyl CH₃) 3.10 (d, ³J_{HH} = 7.0, 1H, allyl CH₂), 3.41 (m, 2H, CH₂Cl), 4.47 (s, 1H, Cp*-H) 4.84 (ddd, ³J_{HH} = 13.7, 9.4, 7.0, 1H, allyl CH). ¹³C APT NMR (300 MHz, C₆D₆): δ 9.1, 10.9 (C₅Me₄H), 12.0 (WCH₂), 17.7 (allyl CH₃), 31.4, 39.8, (chlorobutyl CH₂), 44.9 (CH₂Cl), 53.2 (allyl CHCH₃), 72.9 (allyl CH₂), 98.7 (C₅Me₄H), 105.7, 106.8, 107.2, 108.3 (Cp*Me₄), 110.1 (allyl CH). MS (LREI, probe temp 100 °C, m/z): 481 [M⁺]. Anal. Calcd for C₁₈H₃₀ClNO: C, 42.39; H, 5.86; N, 2.91. Found: C, 40.86; H, 5.69; N, 2.89. Elemental analysis for carbon content was consistently lower than the calculated value. This may be due to incomplete combustion of the solid.

Thermolysis of Cp*W(NO)(CH₂CMe₃)(η³-CH₂CHCHPh) (7*) in Benzene: Preparation of Cp*W(NO)(H)(η³-PhCCCHCHPh) (9*). A Kontes flask was charged with **7*** (53.7 mg, 0.100 mmol) and benzene (2 mL). The mixture was degassed at a vacuum line with three freeze-pump-thaw cycles, and the flask was placed in a 75 °C water-ethylene glycol bath for 1 day. The volatiles were removed in vacuo from the final reaction mixture, and the yellow-brown residue was redissolved in pentane. The pentane solution was transferred to the top of an alumina column (6 × 0.5 cm) supported on glass wool in a Pasteur pipet. A light yellow band was eluted from the column with 1/1 Et₂O/pentane as eluent and was collected. Concentration of the eluate followed by storage at -30 °C for 1 day induced the deposition of Cp*W(NO)(H)(η³-PhCCCHCHPh) (**9***) as yellow needles (42 mg, 75% yield).

Characterization Data for 9*. IR (cm⁻¹): 1564 (s, ν_{NO}). ¹H NMR (400 MHz, C₆D₆): δ -0.15 (s, ¹J_{WH} = 124, 1H, WH), 1.61 (s, 15H, C₅Me₃), 2.02 (d, ³J_{HH} = 10.0, 1H, allyl PhCH), 2.74 (m, ³J_{HH} = 12.6, 1H, allyl PhCH), 5.90 (dd, ³J_{HH} = 12.6, 10.0, 1H, allyl CH), 7.00 (t, ³J_{HH} = 7.6, 1H, para CH), 7.09 (t, ³J_{HH} = 7.6, 1H, para CH), 7.16 (obscured, m, 2H meta CH), 7.33 (overlapping m, 4H, ortho and meta CH), 7.55 (d, ³J_{HH} = 7.6, 2H, ortho CH). ¹³C APT (100 MHz, C₆D₆): δ 10.2 (C₅Me₃), 62.7 (allyl PhCH), 75.6 (allyl PhCH), 103.9 (allyl CH), 105.0 (C₅Me₃), 125.3, 126.4, 127.1, 128.6, 128.7 (aryl C), 143.0, 145.1 (ipso C). MS (LREI, probe temperature 100 °C, m/z): 543 [M⁺]. Anal. Calcd for C₂₅H₂₉NOW: C, 55.26; H, 5.38; N, 2.58. Found: C, 55.16; H, 5.28; N, 2.54.

Preparation of Cp*W(NO)(CH₂CMe₃)(η³-CH₂CHCHPh) (7'). A Schlenk flask was charged with Cp*W(NO)Cl₂ (2.700 g, 6.65 mmol) and (CH₂CMe₃)₂Mg·x(dioxane) (titer 126 g/mol of R, 0.63 g, 4.94 mmol of R). THF (ca. 50 mL) was cannulated into the Schlenk flask at -196 °C, and the mixture was warmed in a dry ice/acetone bath at -78 °C. A red solution first formed and then darkened to a black-red

The THF was removed under reduced pressure to obtain a dark red oily residue. A second Schlenk flask was charged with (CH₂CHCHPh)₂Mg·x(dioxane) (titer 2340 mL/mol of R, 11.6 mL, 4.96 mmol of R). The red oil in the first Schlenk flask was dissolved in Et₂O, and the solution was cannulated over to the second Schlenk flask at -78 °C. The reaction mixture was stirred for 1 h, whereupon a dark red solution was obtained. The solvent was removed in vacuo to obtain a dark red residue. The residue was dissolved in 1/1 pentane/Et₂O, and the solution was chromatographed on an alumina column (2 × 6 cm). A pale red band was eluted from the column, and the eluate was concentrated in vacuo to a red oil which was recrystallized from pentane at -30 °C overnight to obtain X-ray-quality crystals of **7'** (250 mg, 9.7% yield).

Characterization Data for 7'. IR (cm⁻¹): 1600 (s, ν_{NO}). ¹H NMR (400 MHz, C₆D₆): δ 1.28 (s, 9H, CH₂CMe₃), 1.33 (s, 6H, C₅Me₄H), 1.40 (s, 3H, C₅Me₄H), 1.49 (s, 3H, C₅Me₄H), 2.50 (br s, 1H, allyl CHPh), 3.63 (br s, 1H, allyl CH₂), 4.63 (s, 1H, C₅Me₄H), 5.61 (br s, 1H, allyl CH), 7.05–7.25 (m, 5H, aryl H). ¹³C APT NMR (100 MHz, C₆D₆): δ 10.0 (C₅Me₄H), 11.1 (C₅Me₄H), 20.1 (CH₂CMe₃), 35.1 (CH₂CMe₃), 39.4 (CH₂CMe₃), 126.4 (aryl C), 127.2 (aryl C), 128.5 (aryl C), 140.1 (ipso C). MS (LREI, m/z, probe temperature 150 °C): 523 [M⁺, ¹⁸⁴W]. Anal. Calcd for C₂₃H₃₃NOW: C, 52.78; H, 6.36; N, 2.68. Found: C, 53.59; H, 6.18; N, 2.70.

Thermolysis of Cp*W(NO)(CH₂CMe₃)(η³-CH₂CHCHPh) (7') in Benzene: Preparation of Cp*W(NO)(C₆H₅)(η³-CH₂CHCHPh) (8'). A sample of **7'** (302 mg, 0.577 mmol) was dissolved in benzene (ca. 5 mL) to obtain a deep orange solution that was transferred into a Kontes flask. The solution was heated to 55 °C in a water/ethylene glycol bath for 22 h. The solvent was then removed in vacuo to obtain an orange oil that was washed with pentane and transferred to the top of an alumina column (0.5 × 5 cm). An orange band was developed with pentane and eluted from the column with Et₂O. The solvents were removed from the combined eluates in vacuo to obtain **8'** as an orange solid (32 mg, 11% yield).

Characterization Data for 8'. IR (cm⁻¹): 1578 (s, ν_{NO}). ¹H NMR (600 MHz, C₆D₆): δ 1.18 (C₅Me₄H), 1.38 (C₅Me₄H), 1.41 (C₅Me₄H), 1.43 (C₅Me₄H), 2.21 (d, ³J_{HH} = 12.9, 1H, allyl CH₂), 2.67 (d, ³J_{HH} = 10.6, 1H, allyl CHPh), 3.48 (d, ³J_{HH} = 7.4, 1H, allyl CH₂), 4.68 (s, 1H, C₄Me₄CH), 5.72 (ddd, ³J_{HH} = 12.9, 10.6, 7.4, 1H, meso H), 7.14 (m, 2H, aryl H), 7.24 (t, ³J_{HH} = 7.3, 2H, aryl H), 7.27 (t, ³J_{HH} = 7.3, 2H, aryl H), 7.32 (m, 1H, aryl H), 7.33 (m, 1H, aryl H), 7.74 (d, ³J_{HH} = 7.3, 2H, aryl H). ¹³C APT NMR (150 MHz, C₆D₆): δ 9.7 (C₄Me₄CH), 10.2 (C₄Me₄CH), 10.8 (C₄Me₄CH), 11.4 (C₄Me₄CH), 64.6 (allyl CHPh), 72.1 (allyl CH₂), 104.4 (C₄Me₄CH), 105.9 (C₄Me₄CH), 106.4 (C₄Me₄CH), 107.9 (C₄Me₄CH), 111.1 (meso C), 114.2 (C₄Me₄CH), 124.3 (aryl CH), 128.1 (aryl CH), 129.01 (aryl CH), 129.07 (aryl CH), 129.10 (aryl CH), 141.7 (allyl ipso C), 143.4 (aryl CH), 156.8 (phenyl ipso C). MS (LREI, m/z, probe temperature 120 °C): 529 [M⁺, ¹⁸⁴W]. HRMS-EI (m/z): [M⁺] calcd for ¹⁸⁴WC₂₄H₂₇NO 529.160 22, found 529.160 53; calcd for ¹⁸²WC₂₄H₂₇NO 527.157 49, found 527.156 87.

Thermolysis of Cp*W(NO)(CH₂CMe₃)(η³-CH₂CHCHPh) (7') in Benzene: Preparation of Cp*W(NO)(H)(η³-PhCCCHCHPh) (9'). A sample of **7'** (204 mg, 0.390 mmol) was dissolved in benzene (ca. 5 mL) and transferred into a Kontes flask to give an orange solution. The solution was heated to 55 °C in a water/ethylene glycol bath for 6 days, after which time the solvent was removed under reduced pressure to obtain **9'** as an orange solid (82 mg, 40% yield).

Characterization Data for 9'. IR (cm⁻¹): 1587 (s, ν_{NO}). ¹H NMR (400 MHz, C₆D₆): δ -0.08 (s, ¹J_{WH} = 10.2, 1H, W-H), 1.56 (s, 3H, C₅Me₄H), 1.58 (s, 3H, C₅Me₄H), 1.59 (s, 3H, C₅Me₄H), 1.66 (s, 3H, C₅Me₄H), 2.24 (d, ³J_{HH} = 10.2, 1H, allyl CH), 2.90 (d, ³J_{HH} = 12.5, 1H, allyl CH), 4.68 (s, 1H, C₅Me₄H), 5.90 (dd, ³J_{HH} = 10.2, 12.5, meso H), 7.01 (t, ³J_{HH} = 7.4, 1H, aryl H), 7.08 (t, ³J_{HH} = 7.4, 2H, aryl H), 7.26 (t, ³J_{HH} = 7.4, 1H, aryl H), 7.31 (t, ³J_{HH} = 7.8, 2H, aryl H), 7.34 (d, ³J_{HH} = 7.8, 2H, aryl H), 7.51 (d, ³J_{HH} = 7.8, 2H, aryl H). ¹³C APT NMR (100 MHz, C₆D₆): δ 10.5 (C₅Me₄H), 11.5 (C₅Me₄H), 11.9 (C₅Me₄H), 12.3 (C₅Me₄H), 61.5 (allyl CH), 74.7 (allyl CH), 93.8 (C₅Me₄H), 104.0 (meso C), 105.3 (C₅Me₄H), 106.3 (C₅Me₄H), 106.6 (C₅Me₄H), 108.1 (C₅Me₄H), 126.75 (aryl CH), 126.80 (aryl CH),

Table 2. X-ray Crystallographic Data for Complexes 2', 2a*, 4*, 9*, and 7'

	2'	2a*	4*	9*	7'
Crystal Data					
empirical formula	C ₁₉ H ₂₅ NOW	C ₂₀ H ₂₇ NOW	C ₂₀ H ₂₇ NOW	C _{27.5} H ₃₅ NOW	C ₂₃ H ₃₃ NOW
cryst habit, color	needle, yellow	plate, orange	plate, yellow	rectangular, yellow	block, orange
cryst size (mm)	0.05 × 0.20 × 0.70	0.10 × 0.20 × 0.30	0.15 × 0.20 × 0.52	0.40 × 0.20 × 0.12	0.25 × 0.15 × 0.15
cryst syst	orthorhombic	triclinic	orthorhombic	orthorhombic	monoclinic
space group	<i>Pbca</i>	$\bar{P}1$	<i>Pbca</i>	<i>P2₁2₁2₁</i>	<i>P2₁/c</i>
<i>V</i> (Å ³)	6961.9(6)	909.55(17)	3663.9(4)	4812.5(10)	2084.45(15)
<i>a</i> (Å)	14.2940(8)	8.4341(9)	9.3285(6)	9.3219(9)	15.8750(7)
<i>b</i> (Å)	13.8238(7)	8.4965(9)	15.5488(9)	22.502(3)	10.3935(4)
<i>c</i> (Å)	35.2329(17)	14.4435(15)	25.2601(16)	22.943(3)	13.9479(6)
α (deg)	90	85.138(5)	90	90	90
β (deg)	90	88.498(5)	90	90	115.076(2)
γ (deg)	90	61.891(4)	90	90	90
<i>Z</i>	16	2	8	8	4
calcd density (Mg/m ³)	1.783	1.757	1.745	1.599	1.668
abs coeff (mm ⁻¹)	6.639	6.335	6.310	4.819	5.553
<i>F</i> ₀₀₀	3648	472	1888	2312	1040
Data Collection and Refinement					
no. of measd rflns					
total	39 364	21 333	27 804	38 299	49 55
unique	9277	5994	6792	11 491	49 55
final <i>R</i> indices ^a					
<i>R</i> ₁	0.0253	0.0377	0.0270	0.0528	0.0326
<i>wR</i> ₂	0.0499	0.0872	0.0589	0.1140	0.0841
goodness of fit on <i>F</i> ^{2b}	1.287	1.226	1.010	1.075	1.026
largest diff peak, hole (e Å ⁻³)	1.575, -1.609	9.664, -5.073	2.985, -1.893	3.745, -2.270	1.580, -1.814
^a <i>R</i> ₁ on <i>F</i> = $\sum(F_o - F_c)/\sum F_o $; <i>wR</i> ₂ = $[(\sum(F_o^2 - F_c^2)^2)/\sum w(F_o^2)^2]^{1/2}$; <i>w</i> = $[\sigma^2 F_o^2]^{-1}$. ^b GOF = $[\sum(w(F_o - F_c)^2)/(\text{degrees of freedom})]^{1/2}$.					

127.0 (aryl CH), 127.3 (aryl CH), 129.06 (aryl CH), 129.08 (aryl CH), 143.27 (ipso C), 143.33 (ipso C). MS (LREI, *m/z*, probe temperature 150 °C): 529 [M⁺]. HRMS-EI (*m/z*): [M⁺] calcd for ¹⁸⁴WC₂₄H₂₇NO 529.160 22, found 529.159 33.

Extended Thermolysis of 7* in Methylcyclohexane: Preparation of Cp*W(NO)(η³-C₇H₁₁)(H) (11*) and Cp*W(NO)(H)(η³-CH(CH₂C₆H₁₁)CHCHPh) (12*). A Kontes flask was charged with 7* (66 mg, 0.12 mmol) and methylcyclohexane (ca. 5 mL) to give an orange suspension. The mixture was placed in a 55 °C water/ethylene glycol bath for 4 days, whereupon it darkened in color. The volatiles were removed in vacuo from the reaction mixture, and the resulting residue was redissolved in a minimum of pentane and transferred to the top of an alumina column (0.5 × 5 cm). An orange band was developed with pentane and eluted with Et₂O. The solvents were removed from the dark orange eluate under reduced pressure to obtain a mixture of complexes 11* and 12* (31 mg, 53% yield). Complex 11* was identified in the crude reaction mixture by comparison of its ¹H NMR spectrum to that previously reported.¹²

Characterization Data for 12*. IR (cm⁻¹): 1576 (s, ν_{NO}). ¹H NMR (600 MHz, C₆D₆): δ -1.10 (s, ¹J_{WH} = 119.2, 1H, W-H), 1.35 (obscured m, 1H, cyclic CH), 1.50 (m, 6H, cyclic CH), 1.58 (m, 2H, cyclic CH), 1.69 (s, 15H, C₅Me₅), 1.77 (obscured m, 2H, cyclic CH), 1.81 (d, ³J_{HH} = 9.7, 1H, allyl CH), 2.03 (d, ³J_{HH} = 13.2, 1H, allyl CH), 5.20 (dd, ³J_{HH} = 9.7, 13.2, 1H, meso H), 7.08 (t, ³J_{HH} = 7.4, 1H, aryl H), 7.31 (t, ³J_{HH} = 7.7, 2H, aryl H), 7.51 (d, ³J_{HH} = 7.5, 2H, aryl H). ¹³C APT NMR (150 MHz, C₆D₆): δ 10.7 (C₅Me₅), 23.3 (cyclic CH₂), 23.7 (cyclic CH₂), 27.0 (cyclic CH₂), 33.4 (cyclic CH₂), 35.7 (cyclic CH₂), 41.8 (cyclic CH₂), 42.1 (cyclic CH₂), 61.5 (allyl CH), 96.6 (allyl CH), 100.5 (meso C), 104.8 (C₅Me₅), 125.5 (aryl CH), 127.5 (aryl CH), 129.0 (aryl CH), 144.1 (ipso). MS (LREI, *m/z*, probe temperature 150 °C): 563 [M⁺]. HRMS-EI (*m/z*): [M⁺] calcd for ¹⁸²WC₂₆H₃₇NOL 561.235 74, found 561.235 22.

Extended Thermolysis of Cp*W(NO)(CH₂CMe₃)(η³-CH₂CHCHPh) (7*) in Ethylcyclohexane: Preparation of Cp*W(NO)(H)(η³-C₇H₁₃) Isomers 14a*,b*. In a glovebox a sample of 7* was suspended in ethylcyclohexane, and the suspension was

transferred to a Kontes flask. The mixture was heated at 55 °C in a water/ethylene glycol bath for 4 days. The solvent was removed from the final mixture in vacuo, and the resulting residue was dissolved in C₆D₆. Complexes 14a*,b* were identified by comparison of their ¹H NMR spectra with those previously reported.¹²

¹H NMR: 14a*, δ -0.92 (s, ¹J_{WH} = 125 Hz, 1H, WH), 1.71 (s, 15H, C₅Me₅), 2.66 (dd, ³J_{HH} = 7.83, 13.30, 1H, allyl CH); 14b*, δ -0.71 (s, 1H, WH), 1.76 (s, 15H, C₅Me₅), 2.69 (dd, ³J_{HH} = 7.43, 11.74, 1H, allyl CH).

Thermolysis of Cp*W(NO)(CH₂CMe₃)(η³-CH₂CHCMe₂) in *n*-Pentane: Preparation of Cp*W(NO)(H)(η³-C₅H₉) Isomers 15a*,b*. A sample of Cp*W(NO)(CH₂CMe₃)(η³-CH₂CHCMe₂) (85 mg, 0.17 mmol) was dissolved in pentane (ca. 5 mL) to produce a bright orange solution. The contents were transferred to a glass reaction flask equipped with a Kontes greaseless stopcock. The reaction mixture was placed in an ethylene/glycol heating bath and heated at 55 °C for 6 h to obtain a brown solution. Solvents were removed in vacuo, and the remaining brown residue was dissolved in pentane and transferred to the top of an alumina column (0.5 × 5 cm) made up in pentane. A yellow band was eluted with 1/1 pentane/Et₂O to give a yellow eluate that was taken to dryness under reduced pressure to obtain Cp*W(NO)(H)(η³-C₅H₉) as a yellow solid (42 mg, 58% yield). A ¹H NMR spectrum of the final mixture in C₆D₆ revealed diagnostic signals attributable to two prominent isomers, 15a*,b*.

¹H NMR: 15a*, δ -1.39 (s, ¹J_{WH} = 121.2, 1H, W-H), 1.75 (s, 15H, C₅Me₅), 4.59 (ddd, ³J_{HH} = 7.4, 10.6, 12.5, 1H, meso H); 15b*, δ -0.83 (s, ¹J_{WH} = 122.0, 1H, W-H), 1.73 (s, 15H, C₅Me₅), δ 4.44 (dd, ³J_{HH} = 9.8, 12.5, 1H, meso H). MS (LREI, *m/z*, probe temperature 150 °C): 419 [M⁺].

X-ray Crystallography. Data collection was carried out at -100 °C on a Rigaku AFC7/ADSC CCD diffractometer or at -170 ± 2 °C on a Bruker X8 or DUO APEX diffractometer, using graphite-monochromated Mo Kα radiation.

Data for 2' (mixture of 2a' and 2b') were collected to a maximum 2θ value of 58.4° in 0.5° oscillations. The structure was solved by

direct methods¹⁴ and expanded using Fourier techniques. All non-hydrogen atoms were refined anisotropically, and all hydrogen atoms were included in fixed positions. The final cycle of full-matrix least-squares analysis was based on 9277 observed reflections and 407 variable parameters.

Data for **2a*** were collected to a maximum 2θ value of 63.3° in 0.5° oscillations. The structure was solved by direct methods¹⁴ and expanded using Fourier techniques. All non-hydrogen atoms were refined anisotropically, and all hydrogen atoms were included in fixed positions. The final cycle of full-matrix least-squares analysis was based on 5994 observed reflections and 214 variable parameters.

Data for **4*** were collected to a maximum 2θ value of 66.4° in 0.5° oscillations. The structure was solved by direct methods¹⁴ and expanded using Fourier techniques. All non-hydrogen atoms were refined anisotropically; hydrogen atom H1 was refined isotropically, and all other hydrogen atoms were included in fixed positions. The final cycle of full-matrix least-squares analysis was based on 6792 observed reflections and 218 variable parameters.

Data for **9*** were collected to a maximum 2θ value of 56.3° in 0.5° oscillations. The structure was solved by direct methods¹⁴ and expanded using Fourier techniques. The structure was a two-component twin. The asymmetric unit contained two independent molecules of **7*** and a disordered pentane. Atom O2 was disordered over two sites in a 52/48 ratio. The pentane was refined anisotropically, but its disorder was not modeled. All non-hydrogen atoms were refined anisotropically. Hydrogens H01 and H02 were refined isotropically and their respective W–H distances and isotropic displacement parameters constrained to be the same. All other hydrogen atoms were included in fixed positions. The final cycle of full-matrix least-squares analysis was based on 11 491 observed reflections and 580 variable parameters.

Data for **7'** were collected to a maximum 2θ value of 55.8° in 0.5° oscillations. The structure was solved by direct methods¹⁴ and expanded using Fourier techniques. The structure was a two-component twin that was separated into its components using Cell_Now,¹⁵ SAINTPLUS,¹⁶ and TWINABS.¹⁷ All non-hydrogen atoms were refined anisotropically, and all hydrogen atoms were included in fixed positions. The final cycle of full-matrix least-squares analysis was based on 4955 observed reflections and 242 variable parameters.

For each structure neutral-atom scattering factors were taken from Cromer and Waber.¹⁸ Anomalous dispersion effects were included in F_o ; the values for $\Delta f'$ and $\Delta f''$ were those of Creagh and McAuley.²⁰ The values for mass attenuation coefficients are those of Creagh and Hubbell.²¹ All calculations were performed using SHELXL-97²² via the WinGX interface.²³ X-ray crystallographic data for all five structures are presented in Table 2, and full details of all crystallographic analyses are provided in the Supporting Information.

■ ASSOCIATED CONTENT

■ Supporting Information

CIF files providing full details of the crystallographic analyses of complexes **2'**, **2a***, **4***, **9***, and **7'**. This material is available free of charge via the Internet at <http://pubs.acs.org>.

■ AUTHOR INFORMATION

Corresponding Author

*E-mail: legzdins@chem.ubc.ca.

■ ACKNOWLEDGMENTS

We are grateful to The Dow Chemical Co. for continuing support of this work, and we thank Drs. Pete Nickias and Brandon Rodriguez for assistance and helpful discussions. We also acknowledge the staff of the UBC High-Resolution NMR facility, specifically Maria Ezhova and Zorana Danilovic, for their assistance in obtaining the 600 MHz NMR spectra and

Dr. Miriam Buschhaus for her assistance with the X-ray crystallography.

■ REFERENCES

- (1) See, for example: (a) Crabtree, R. H. *J. Chem. Soc., Dalton Trans.* **2001**, 17, 2437. (b) Labinger, J. A.; Bercaw, J. E. *Nature* **2002**, 417, 507. (c) Goldman, A., Goldberg, K. I., Eds. *Activation and Functionalization of C–H Bonds*; American Chemical Society: Washington, DC, 2004. (d) Fekl, U.; Goldberg, K. I. *Adv. Inorg. Chem.* **2003**, 54, 259. (e) Hartwig, J. F. *Organotransition Metal Chemistry: From Bonding to Catalysis*; University Science Books: Sausalito, CA, 2010; Chapter 18.
- (2) Tsang, J. Y. K.; Buschhaus, M. S. A.; Fujita-Takayama, C.; Patrick, B. O.; Legzdins, P. *Organometallics* **2008**, 27, 1634.
- (3) For recent examples of the selective functionalization of C–H bonds, see: Crabtree, R. H. *Chem. Rev.* **2010**, 110, 575 and the reviews in this special issue.
- (4) Ng, S. H. K.; Adams, C. S.; Hayton, T. W.; Legzdins, P.; Patrick, B. O. *J. Am. Chem. Soc.* **2003**, 125, 15210.
- (5) Tsang, J. Y. K.; Buschhaus, M. S. A.; Graham, P. M.; Semiao, C. J.; Semproni, S. P.; Kim, S. J.; Legzdins, P. *J. Am. Chem. Soc.* **2008**, 130, 3652.
- (6) Baillie, R. A.; Man, R. W. Y.; Shree, M. V.; Chow, C.; Thibault, M. E.; McNeil, W. S.; Legzdins, P. *Organometallics* **2011**, 30, 6201.
- (7) Baillie, R. A.; Tran, T.; Thibault, M. E.; Legzdins, P. *J. Am. Chem. Soc.* **2010**, 132, 15160.
- (8) Throughout this report the compounds being studied are designated by bold numbers or letters. The symbols * and ' after the numbers or letters indicate the Cp*- and Cp'-containing complexes, respectively. If no symbol is shown, then the designation encompasses both the Cp* and the Cp' compounds.
- (9) As described in the Experimental Section, Cp'W(NO)(CH₂CMe₃)(η^3 -CH₂CHCHMe) can be synthesized in moderate yields by utilizing the procedure reported for its Cp* analogue.⁵
- (10) Semproni, S. P.; McNeil, W. S.; Baillie, R. A.; Patrick, B. O.; Campana, C. F.; Legzdins, P. *Organometallics* **2010**, 29, 867.
- (11) Related η^3 -H₂CCHCMe₂ complexes also exhibit exo orientations of their allyl ligands.⁴
- (12) Adams, C. S.; Legzdins, P.; Tran, E. *J. Am. Chem. Soc.* **2001**, 123, 612.
- (13) Pamplin, C. B.; Legzdins, P. *Acc. Chem. Res.* **2003**, 36, 223.
- (14) SIR-92: Altomare, A.; Cascarano, G.; Giacovazzo, C.; Guagliardi, A. *J. Appl. Crystallogr.* **1993**, 26, 343.
- (15) Cell_Now 2008/2; Bruker AXS Inc., Madison, WI.
- (16) SAINTPLUS, Version 7.60A; Bruker AXS Inc., Madison, WI, 1997–2008.
- (17) TWINABS, V2008/2; Bruker AXS Inc., Madison, WI, 2007.
- (18) Cromer, D. T.; Waber, J. T. *International Tables for X-ray Crystallography*; Kynoch Press: Birmingham, U.K., 1974; Vol. IV, Table 2.2A.
- (19) Ibers, J. A.; Hamilton, W. C. *Acta Crystallogr.* **1964**, 17, 781.
- (20) Creagh, D. C.; McAuley, W. J. *International Tables for X-ray Crystallography*; Kluwer Academic: Boston, 1992; Vol. C, Table 4.2.6.8.
- (21) Creagh, D. C.; Hubbell, J. H. *International Tables for X-ray Crystallography*; Kluwer Academic: Boston, 1992; Vol. C, Table 4.2.4.3.
- (22) SHELXL-97: Sheldrick, G. M. *Acta Crystallogr.* **2008**, A64, 112.
- (23) WinGX-V1.70: Farrugia, L. J. *J. Appl. Crystallogr.* **1999**, 32, 837.